GEOLOGICA CARPATHICA, JUNE 2023, 74, 3, 245–260 https://doi.org/10.31577/GeolCarp.2023.12

Geochronology and petrogenesis of the lower Miocene felsic rocks: New evidence for initiation of post-collisional magmatism in the SW Malatya – Eastern Anatolia (Turkey)

MEHMET ALI ERTÜRK[1,✉], HATICE KARA[1], ABDULLAH SAR[1], İSAK YILMAZ[2] and NAMIK AYSAL[2]

[1]Fırat University, Department of Geological Engineering, 23119, Elazığ, Turkey; ✉erturkmae@gmail.com
[2]İstanbul University-Cerrahpasa, Department of Geological Engineering, İstanbul, Turkey

(Manuscript received June 20, 2022; accepted in revised form May 18, 2023; Associate Editor: Milan Kohút)

Abstract: The Southeast Anatolian Orogenic Belt (SAOB) consists of various tectono-magmatic and tectono-stratigraphic units such as metamorphic massifs, granitoids, ophiolites and volcanic rocks. In this study, we report new zircon U–Pb LA-ICP-MS ages, Sr–Nd isotope analysis and whole-rock geochemistry from Miocene felsic (dacitic and rhyolitic) rocks cross-cutting the Permo–Triassic Malatya metamorphic complex to determine the source of magmatism and magmatic processes in the region. The zircon U–Pb crystallisation ages are between 16.66±0.23 Ma and 16.83±0.094 Ma, implying the start of the post-collisional volcanism in the Early Miocene (Burdigalian) period. Volcanic rocks have calc-alkaline and high-K calc-alkaline characters. The $^{87}Sr/^{86}Sr$ values for the felsic volcanics range between 0.707098 and 0.711703. The initial $^{143}Nd/^{144}Nd$ ratios are between 0.512446 and 0.512469, and the εNd values vary from −3.12 to −3.66. The Nd (T_{DM}) model ages are between 1.05 and 1.13 Ga. Negative εNd values and Nd (T_{DM}) model ages show great similarities with the Precambrian basement in Turkey, Iran and the Arabian peninsula. Energy-constrained assimilation–fractional crystallisation (EC-AFC) models testing different crustal sources using Sr–Nd isotope data show that primary magmas contain significant crustal melt contributions. Geochemical data indicate that the felsic rocks may have originated from crust-derived melts mixed with lithospheric mantle-derived mafic melts during its residence in the upper crust in a post-collisional tectonic setting.

Keywords: felsic rocks, zircon U–Pb ages, lithospheric mantle, upper crust, post-collisional volcanism, Eastern Turkey

Introduction

The Eastern Anatolian Volcanic Province (EAVP), one of the best samples of post-collisional magmatism, has been active since the early Miocene (Şengör & Yılmaz 1981). Recent studies show that the onset of volcanic activity covering large areas is older than the middle-late Miocene. A number of studies have been conducted to place constraints on the geochemical, petrological and geochronological characteristics of the subduction-related or post-collisional tectonic setting of Cenozoic volcanism in EAVP, Yamadağ Volcanic Complex (YVC) and Arabian Foreland (Fig. 1; Leo et al. 1974; Pearce et al. 1990; Arger et al. 2000; Keskin 2003, 2007; Ekici et al. 2007, 2009; Yılmaz et al. 2007; Kürüm et al. 2008, 2021; Önal et al. 2008; Ekici 2016; Di Giuseppe et al. 2017; Karaoğlu et al. 2020; Caran & Polat 2022).

The EAVP is an important part of the Alpine–Himalayan Orogenic Belt (Şengör & Yılmaz 1981; Karaoğlan et al. 2016; Sar et al. 2019; Ertürk et al. 2022). It has a complex geodynamic history, with northward subduction and closure of several branches of the Tethyan Ocean and the merging of several continental blocks lying between them (Şengör & Yılmaz 1981). This belt occupies the extensive and central segment of the 7000 km long Alpine–Himalayan orogenic belt and preserves the records of the subduction-collision processes associated with the Neotethyan Ocean. This belt was named the Eastern Anatolian Collision Zone (EACZ) since it merged due to the collision of the Arabian and Anatolia plates (Pearce et al. 1990; Keskin 2003, 2007). The volcanic activity started with the neotectonic episode during the early Miocene in Eastern Anatolia (Şengör & Yılmaz 1981). Eastern Anatolia comprises several microcontinents amalgamated along an accretionary prism and SE Anatolian ophiolite belts during the closure of the Neo-Tethys Ocean (Şengör et al. 2008). Topuz et al. (2017) proposed that this accretionary prism is absent in Eastern Anatolia, and thinning of the lithosphere is unrelated to the oceanic slab steepening and breaking beneath an accretionary complex. The basement rocks comprise upper Cretaceous high-T/low-P metamorphics and upper Cretaceous gabbroic to tonalitic intrusion rocks (Topuz et al. 2017, 2019). The Oligocene unconformably overlies those microcontinents to Miocene shallow marine deposits and post-collisional late Cenozoic volcanism (Elmas & Yılmaz 2003; Özdemir et al. 2022).

The geodynamic and volcanic evolution of the EAVP is still controversial. Many different models have been proposed for the Cenozoic volcanism in Eastern Anatolia: (i) subduction-related model (Di Giuseppe et al. 2017; Agostini et al. 2019), (ii) collision-related model (Ekici et al. 2009; Ekici 2016; Kürüm et al. 2021), (iii) slab break-off-window and/or delamination (post-collisional) (Keskin 2007; Kürüm et al. 2008;

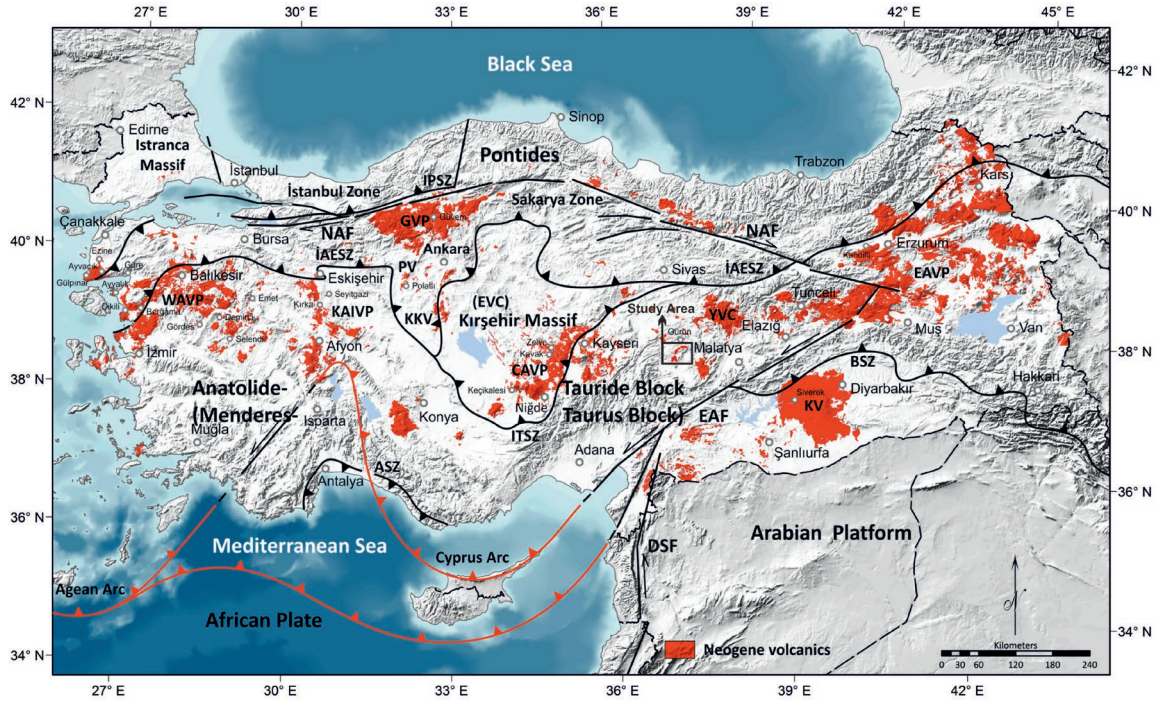

Fig. 1. A simplified tectonic map of Turkey showing the major suture zones (heavy black lines with filled triangles), arc systems (heavy red lines with filled triangles) and continental blocks (Okay & Tüysüz 1999), and distribution of the main Neogene volcanic fields (modified from Asan 2020). EAVP: Eastern Anatolian Volcanic Province, CAVP: Central Anatolian Volcanic Province, GVP: Galatia Volcanic Province, PV: Polatlı Volcanites, EVC: Elmadağ Volcanic Complex, KKV: Kulu-Karacadağ Volcanites, KAIVP: Kırka-Afyon-Isparta Volcanic Province, WAVP: Western Anatolian Volcanic Province, YVC: Yamadağ Volcanic Complex, KV: Karacadağ Volcano, İAESZ: İzmir–Ankara–Erzincan Suture Zone, ITSZ: Inner Tauride Suture Zone, BSZ: Bitlis Suture Zone, IPSZ: Intra-Pontide Suture Zone, ASZ: Antalya Suture Zone, NAF: North Anatolian Fault, EAF: East Anatolian Fault, DSF: Dead Sea Fault.

Schleiffarth et al. 2018; Rabayrol et al. 2019; Topuz et al. 2019, and this study) models.

We present petrographic observations, zircon U–Pb ages, whole-rock geochemistry and Sr–Nd isotope data on the representative samples of the felsic rocks in this study. Many researchers focused on the geodynamic evolution of the SAOB (Kürüm et al. 2008, 2021; Önal et al. 2008; Karaoğlan et al. 2013, 2016; Parlak et al. 2013; Nurlu et al. 2016, 2022; Rizeli et al. 2016, 2021; Ertürk et al. 2017, 2018, 2022; Beyarslan et al. 2018, 2022; Sar et al. 2019, 2022). However, the zircon U–Pb age data on the Miocene volcanic rocks of the Malatya region have been presented for the first time. This study is important for revealing new approaches to controversial geodynamic settings and magma origin in Eastern Anatolia. As a result of this study, a new evaluation was made regarding the beginning of magmatism, magma character and origin of volcanic rocks by evaluating all available data together with the literature and providing new insights to reveal the Cenozoic magmatism in the SAOB.

Geological background

The Eskiköy–Doğanşehir region, situated at the west of Malatya city, consists of the Palaeozoic–Mesozoic Malatya Metamorphic Complex, upper Cretaceous–Eocene Berit metaophiolite, Eocene Maden Complex, early-middle Eocene Doğanşehir pluton, and Plio–Quaternary cover sedimentary units (Ural et al. 2015, 2021, 2022; Karaoğlan et al. 2016; Ertürk et al. 2018; Fig. 2). Malatya metamorphics are composed of mica-schist, quartz–sericite schist, phyllite, dolomite, marble and recrystallised limestone from bottom to top (Önal 1995; Önal & Altunbey 1999; Sağıroğlu et al. 2013; Kara & Sağıroğlu 2018; Kara & Bal Akkoca 2021). Malatya metamorphic Complex was thrust over the ophiolites from north to south during the late Cretaceous (Yazgan & Chessex 1991). The Berit metaophiolite was formed by the northward subduction of the southern branch of Neotethys starting from the late Cretaceous and the opening (supra-subduction zone) of the oceanic plate above the subducted plate (Önal & Beyarslan 2001). This unit comprises serpentinised peridotites, gabbros, and cross-cutting verlitic veins (Karaoğlan et al. 2013). The Maden complex consists of basalt, basaltic andesite, andesite, diabase, and pyroclastic rocks (Ertürk et al. 2018). The Doğanşehir (Malatya) granitoid rocks have typical calc-alkaline, I-type character (Karaoğlan et al. 2013). These rocks formed on the active continental margin (Önal 1995) during 50.8–45.7 Ma (Karaoğlan et al. 2013). The studied volcanic rocks are represented by dacite and rhyolite. They cut the Malatya Metamorphic Complex into rocks with a width of 5–10 meters (Fig. 3). Plio-Quaternary cover sedimentary units are composed of alluvium.

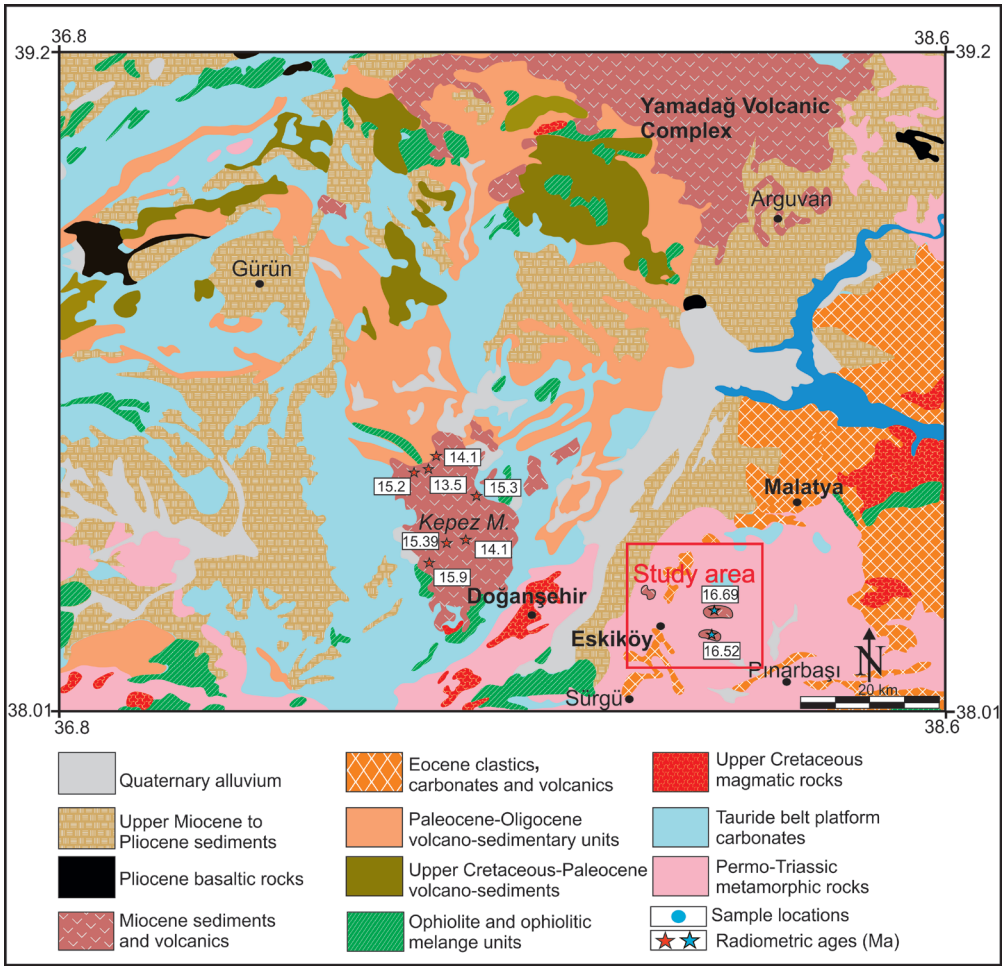

Fig. 2. Simplified geological map of the Sivas–Malatya region (compiled from 1/500,000-scale sheets of Geological Map of Turkey, General Directorate for Mineral Research and Exploration-MTA 2013). Age data: Leo et al. (1974); Platzman et al. (1998); Arger et al. (2000); Kürüm et al. (2008); Önal et al. (2008); Ekici et al. (2009); Gürsoy et al. (2011).

Petrography

Dacitic lavas within the felsic rocks are grey and show fine-grained microcrystalline, vitrophyric, porphyritic, glomeraphyric and hypohyaline porphyritic textures (Fig. 4a, b). The main mineral assemblage comprises plagioclase (30–35 %), quartz (24–30 %), sanidine (3–5 %), biotite (3–5 %) and hornblende (2–5 %) in a microlithic-glassy groundmass. The accessory minerals are represented by titanite, zircon and opaque minerals. Plagioclase phenocrysts demonstrate dissolution textures (sieve texture) related to magma mixing, albite – Carlsbad twinning, and oscillatory zoning. Rhyolites display porphyritic texture and are mainly greyish to pinkish in colour. They comprise quartz (25–30 %), sanidine (21–25 %), plagioclase (20–25 %), biotite (3–5 %) and amphibole (2–5 %). Plagioclase microliths (8–10 %) were disseminated in a partly felsitic glassy groundmass. Zircon, apatite, Fe–Ti oxides (titanite, ilmenite), and opaque minerals are observed in the accessory phase. Sanidine and plagioclase are subhedral and anhedral shapes, showing albite and Carlsbad twinning (Fig. 4c, d).

Analytical methods

Whole-rock major and trace element analyses

Whole-rock chemical compositions were analysed at Bureau Veritas Minerals Laboratories in Vancouver, Canada. Major elements were measured using a Spectro Ciros Vision device inductively coupled plasma atomic emission spectroscopy (ICP-AES). Trace and rare earth elements were measured using a Perkin Elmer Elan DRCe inductively coupled plasma-mass spectrometry (ICP-MS). Loss on ignition (LOI) was calculated by weight difference later ignition of samples at 950–1000 °C. Our results for the whole-rock geochemistry are given in Supplementary Table S1.

Sr–Nd isotope analyses

Sr and Nd isotope compositions were carried out in the METU Central Laboratory, Turkey, by applying in-laboratory test instructions based on the methods detailed and conditions given in Köksal (2019). Isotope ratio measurements were

made by multi-collection using the Triton Thermal Ionization Mass Spectrometer (Thermo-Fisher).

Zircon U–Pb

Two samples (EK-2 and EK-9) were selected for LA-ICP-MS U–Pb zircon dating. Zircon U–Pb analyses were conducted using Perkin Elmer NexION 2000 ICP-MS combined with the ESI NWR-213 solid phase Laser Ablation System present at the Geochronology and Geochemistry Laboratory of Istanbul University – Cerrahpaşa – Turkey, following the analytical methods by Yılmaz et al. (2021).

Results

Geochemistry

The felsic rocks have high SiO_2 content (66.91–73.81 wt.%), relatively low Al_2O_3 (13.54–15.89 wt.%), Fe_2O_3 (0.68–2.72 wt.%), MgO (0.17–1.27 wt.%), CaO (0.87–3.35 wt.%), Na_2O (3.25–3.87 wt.%), K_2O (2.11–5.03 wt.%), TiO_2 (0.07–0.41 wt.%), P_2O_5 (0.02–0.13 wt.%), and varying amounts of Ba (140–470 ppm), Nb (5.2–15.9 ppm), Rb (73.2–227.2 ppm), Sr (38.6–275.1 ppm), Nb/La (0.27–1.71) and Nb/U (1.13–2.35) ratios.

These felsic rocks have sub-alkaline compositions and fall into the dacite–rhyolite fields in the total alkali versus silica (TAS) diagram (Le Bas et al. 1986; Fig. 5a). These are coherent with the field studies and petrographic observations. On the Th versus Co diagram proposed by Hastie et al. (2007), our samples fall into the high-K calc-alkaline and shoshonitic fields with dacitic and rhyolitic compositions (Fig. 5b). Similarly, our samples in the K_2O versus SiO_2 diagram (Peccerillo & Taylor 1976) fall in the calc-alkaline and high-K calc-alkaline fields (Fig. 5c). Eu/Eu* ratios of the rocks vary between 0.73–1.02 with a slightly negative Eu anomaly (Fig. 5d). Selected major and trace elements were plotted on Harker variation diagrams versus SiO_2 abundance (Figs. 6, 7). On primitive mantle-normalised multi-element spidergram (Fig. 8a), dacitic and rhyolitic samples are enriched in Sr, K, Rb, Ba, and Th elements, and to a lesser extent, in La, Ce, and Nd, but depleted in P and Ti elements. The decrease from Th to Ta and Nb is more profound than from La to Nd. On the other hand, Nd, Hf, Sm, Tb, Y, and Yb form an almost horizontal trend, showing weaker enrichment than other elements. In a chondrite-normalised REE diagram (Fig. 8b), LREEs are more enriched than HREEs, and negative Eu anomalies characterise the studied samples.

Sr–Nd isotope systematics

The Sr–Nd isotopic compositions of lower Miocene volcanics are listed in Suppl. Table S2. The initial $^{87}Sr/^{86}Sr_{(i)}$ ratios vary between 0.706927 and 0.709559, and the initial $^{143}Nd/^{144}Nd_{(i)}$ ratios show a narrow range between 0.512430 and 0.512458. The volcanics show negative $\varepsilon Nd_{(t)}$ values ranging from −3.12 to −3.66. The Nd (T_{DM}) model ages range between 1.05 and 1.13 Ga. On the $^{87}Sr/^{86}Sr$ versus $^{143}Nd/^{144}Nd$ diagram, the high Sr isotope values of the rhyolitic lavas are striking, while the dacitic lavas fall into the Arabian Upper crustal field (Fig. 9a). EC-AFC models were tested using Sr–Nd isotope data of upper crust (UC-Model-1), lower crust (LC-Model-2), and Arabian upper crusts (AUC-1 Model-3; AUC-2 Model-4; Sr–Nd isotope data for Arabian upper crusts are from Hegner & Pallister 1989; Fig. 9b).

U–Pb geochronology

The zircons from the EK-2 and EK-9 samples are mostly transparent, colourless, pale-brownish, and rarely beige. They have euhedral to subhedral shapes and elongate to prismatic (50 to 250 μm). They display typical magmatic oscillatory zoning in the CL images (Fig. 10). The Th/U ratios of the zircons from the EK-2 sample vary between 0.14 and 040 (mean 0.23±0.068), and most clusters from 0.14–0.29 show magmatic origin (Grimes et al. 2015). For sample EK-2, thirteen analyses yielded apparent $^{206}Pb/^{238}U$ ages ranging from 14.68±0.87 Ma to 17.45±1.99 Ma (Suppl. Table S3). They have yielded concordia age of 16.66±0.23 Ma (MSWD=11, n=12; Fig. 11a), with a weighted mean $^{206}Pb/^{238}U$ age of 16.36±0.25 Ma (MSWD=0.37, n=13/13; Fig. 11b). The Th/U ratios of the zircon grains of the EK-9 sample vary between 0.08 and 0.79 (mean 0.36), consistent with a magmatic origin (Grimes et al. 2015). The analyses of zircons from sample EK-9 yielded $^{206}Pb/^{238}U$ ages of 15.13±0.45 Ma to 18.5±0.32 Ma (Suppl. Table S3). The twelve analyses yielded concordia age of 16.83±0.094 Ma (MSWD=2.8, Fig. 11c) with a weighted mean $^{206}Pb/^{238}U$ age of 16.45±0.12 Ma (MSWD=2.63, n=10/12; Fig. 11d).

Discussion

Magma chamber processes

In the selected major oxides and trace-element variation diagrams against SiO_2, samples from the studied rocks and volcanic equivalent define a continuous evolutionary trend: Al_2O_3, Fe_2O_3, MgO, CaO, Na_2O, TiO_2 and P_2O_5 are negatively correlated with increasing SiO_2, but the K_2O contents show a positive correlation. Na_2O show a disseminated pattern (Fig. 6). Such positive and negative correlations are associated with the fractional crystallisation process. The observed decrease in Na_2O is related to the fractionation of sodic plagioclase, the decreases in Al_2O_3 with the fractionation of biotite, and negative trends in CaO and MgO with pyroxene fractionation, negative trends in Fe_2O_3 and TiO_2 with amphibole and titanite fractionation, and decreases in P_2O_5 with apatite fractionation (Wilson 1989). A negative relationship is observed with the increase between Ba, Co, Sr and Zr and SiO_2, and a positive relationship between SiO_2 and Rb and Nb

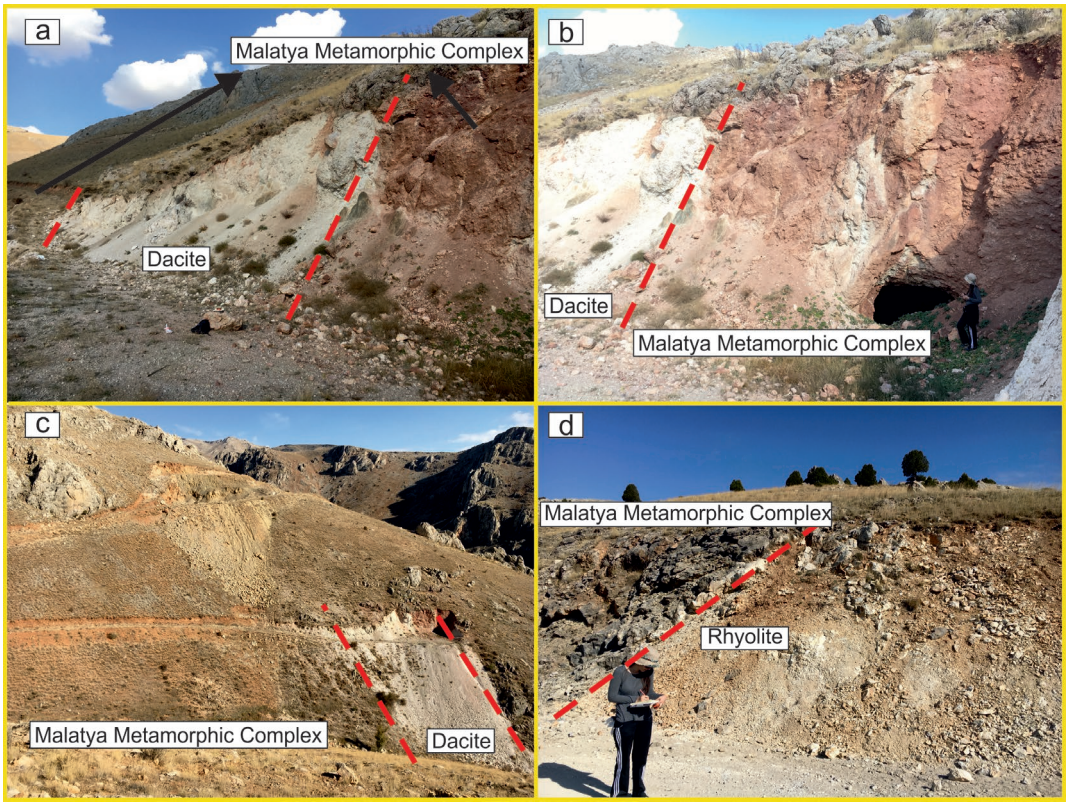

Fig. 3. Representative field photographs of the lower Miocene felsic rocks in the Eskiköy–Doğanşehir (Malatya).

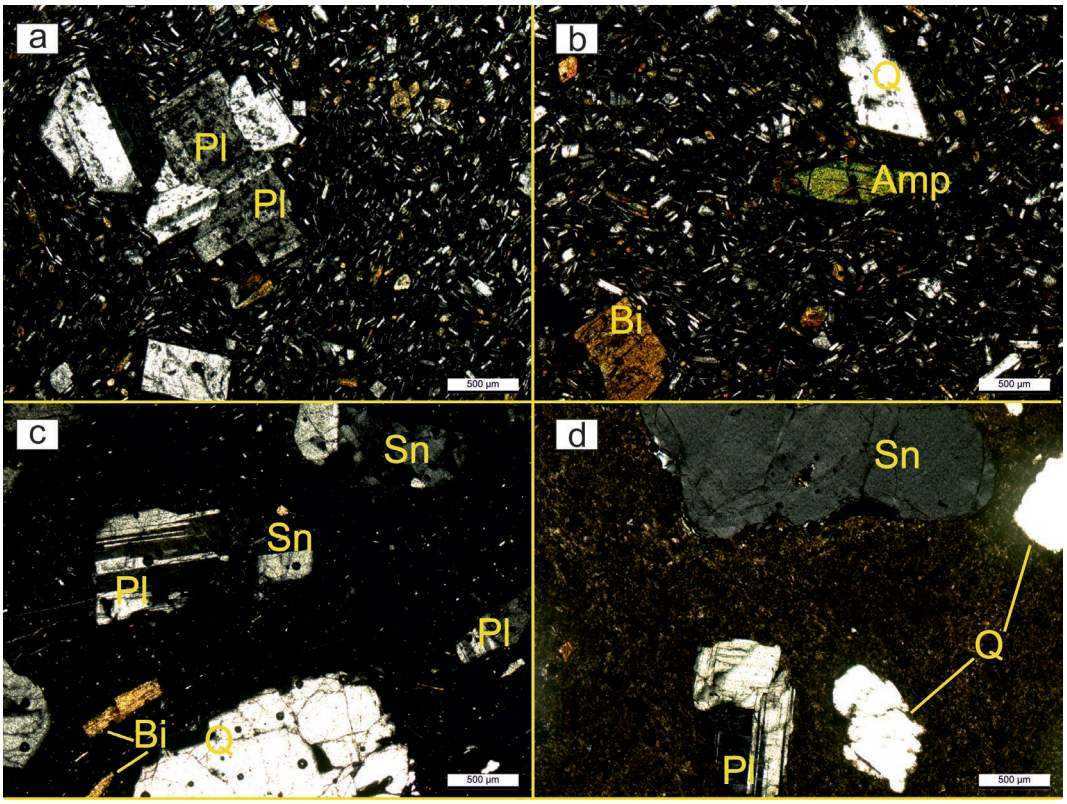

Fig. 4. Photomicrographs of the lower Miocene felsic rocks in the Eskiköy–Doğanşehir (Malatya). **a** — Glomeraphyric texture in dacite. **b** — Hypohyaline porphyric texture in dacite. **c** — Hypohyaline porphyric texture in rhyolite. **d** — Plagioclase, sanidine and quartz phenocrysts in rhyolite (Q: quartz, Sn: sanidine, Pl: plagioclase, Bi: biotite, Hr: hornblende).

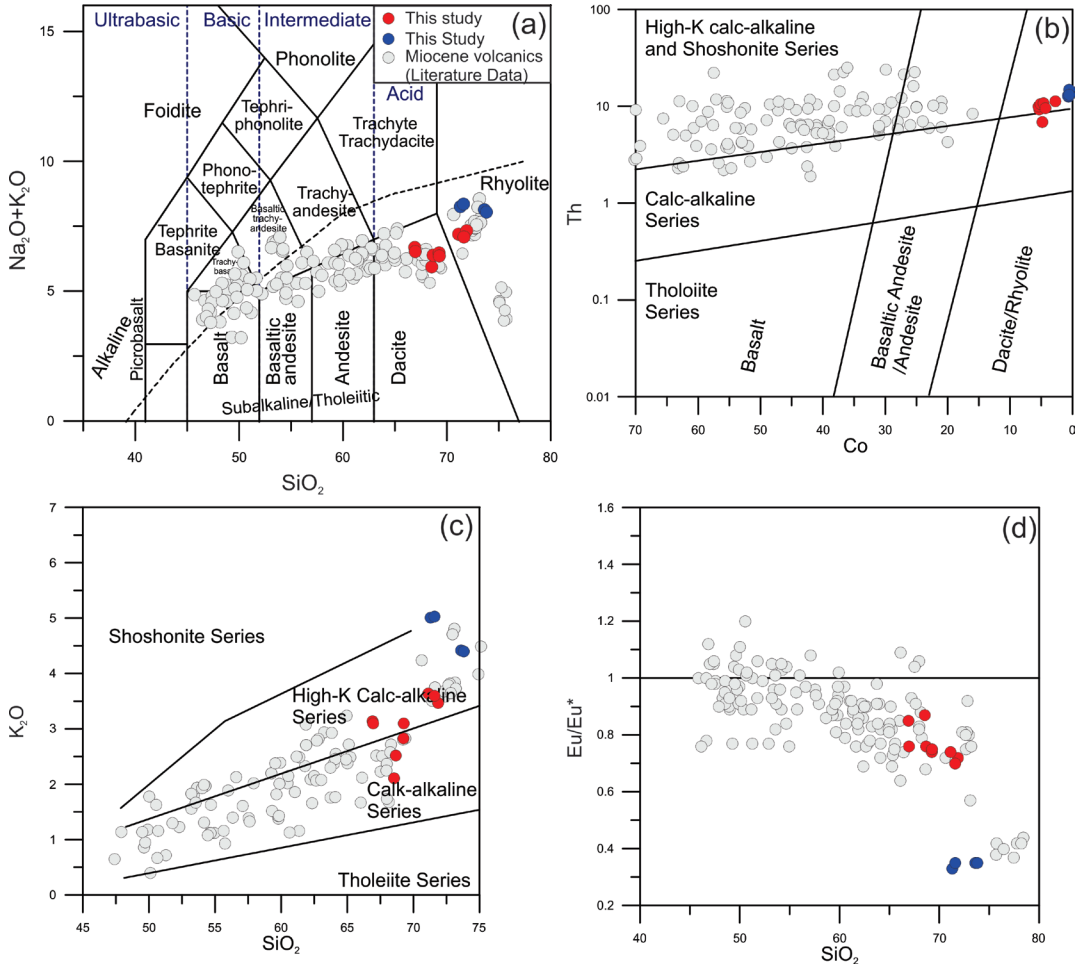

Fig. 5. a — Na_2O+K_2O versus SiO_2 classification diagram of Middlemost (1994). **b** — Th versus Co diagram of Hastie et al. (2007). **c** — K_2O versus SiO_2 diagram of Peccerillo & Taylor (1976). **d** — Eu/Eu* versus SiO_2 diagram. Eu anomalies (Eu/Eu*) have been calculated as $Eu/Eu^*=(Eu)_{cn}/[(Sm)_{cn}\times(Gd)_{cn}]^{0.5}$ from McLennan (1989) normalised with C1 chondrite values (Sun & McDonough 1989). The literature data for Miocene volcanics in the Southeast Anatolian Orogenic Belt are inferred from (Arger et al. 2000; Yılmaz et al. 2007: Kürüm et al. 2008; Önal et al. 2008; Ekici et al. 2009; Ekici 2016; Kocaarslan & Ersoy 2018).

(Fig. 7). Ba, Sr, Co and Zr elements can be incorporated into minerals such as K-feldspar, hornblende, and biotite during fractional crystallisation (Wilson 1989). These minerals positively correlate with SiO_2 during fractional crystallisation as they crystallise at later stages.

The Energy Constrained-Assimilation Fractional Crystallization (EC-AFC) model (Bohrson & Spera 2001) checks the effect of crustal melts on the evolution of magma. The thermal and compositional parameters used in EC-AFC modelling are given in Suppl. Table S4 (Bohrson & Spera 2001). EC-AFC modelling with using Sr–Nd isotopes provides important clues for understanding the crustal assimilation and fractional crystallisation processes, considering the lower crust (LC), upper crust (UC), and Arabian upper crustal rocks muscovite schist (AUC-1), and biotite granite-gneiss (AUC-2) (Hegner & Pallister 1989; Fig. 9b). Miocene basalts in the region were used as the basic end member in the models (Ekici 2016). According to EC-AFC modelling, the assimilation values of dacite and rhyolitic lavas from an upper crust-like source (UC Model-1) are between 7 % and 17 % (Ma* 0.07–0.17); from a source similar to muscovite schists of the Arabian upper crust (AUC-1 Model-3) are between 24 % and 48 % (Ma* 0.24–0.48), and from a source similar to biotite granite gneisses of the Arabian upper crust (AUC-2 Model-4) is 65 % (Ma* 0.65; Fig. 9b). These assimilation values show that the magmas forming the felsic rocks are of crustal origin.

FC Modeller program was used for fractional crystallisation (FC) modelling. Vectors indicating different mineralogical compositions can help us interpret FC processes in magma evolution history. The incompatible element Rb was used against the compatible elements Sr and Ba in the log-log diagram (Fig. 12a, b). As a reflection of the fractional crystallisation of plagioclase in magma, this diagram presents a decrease in Sr values with increasing Rb concentration. In conclusion, it can be highlighted that plagioclase crystallisation compatible with Sr has an essential role in the evolution of the magma chamber. Ba was affected by amphibole and K-feldspar crystallisation. It was incorporated into amphibole and K-feldspars,

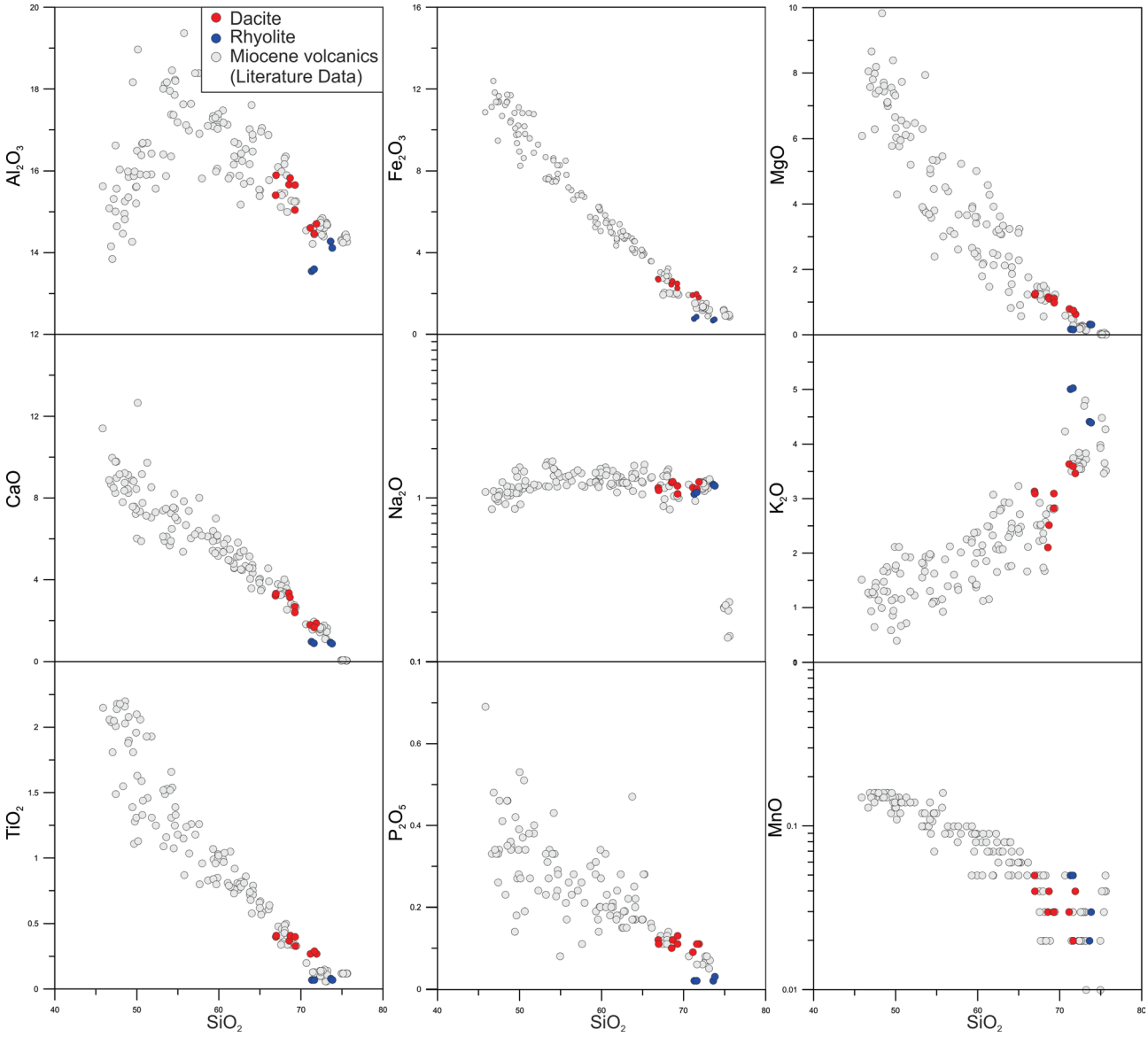

Fig. 6. Variation diagrams of SiO_2 (wt.%) versus major elements (Harker 1909). The literature data is the same as in Fig. 5.

especially in the late stage of magma evolution. A partial increase is observed in Ba values with increasing Rb, and it can be underlined that the crystallisation of amphibole and/or biotite minerals compatible with Ba has an important role in the evolution of the magma chamber.

Petrogenesis and source characteristics

Based on the primitive mantle-normalised multi-element spidergram, large ion lithophile elements (LILE) show more enrichment than high field strength elements (HFSE) (Fig. 8a). The negative Nb, P, Ti and positive Pb anomalies are characteristic of subduction-related magmatism in a volcanic arc and/or post-collisional tectonic settings and originate from a metasomatised mantle by fluids separated from the oceanic crust (Hawkesworth et al. 1993). The enrichment in LILEs can result from fluids or melts derived from the subducting slab being transported upwards (toward the mantle wedge above the subducting slab) and their metasomatised mantle wedge (McDonough 1991). This enrichment results from the reaction of volatile compounds such as H_2O and CO_2 from the relatively lower part of the mantle and LILE-rich fluids/melts with the solid mantle rocks at the higher levels (Menzies 1983). The depletion of HFSEs, on the other hand, occurs when these elements are retained in the mineral phases of the subducting plate (McDonough 1991). Moreover, when the upper and lower crust values are plotted on this diagram, the volcanic rocks appear to be located between both crustal values in the region. However, apart from the significant depletion of P and Ti elements, most elements are located in an area between the upper crust and the lower crust (Fig. 8a). This pattern shows that highly fractionated dacitic and

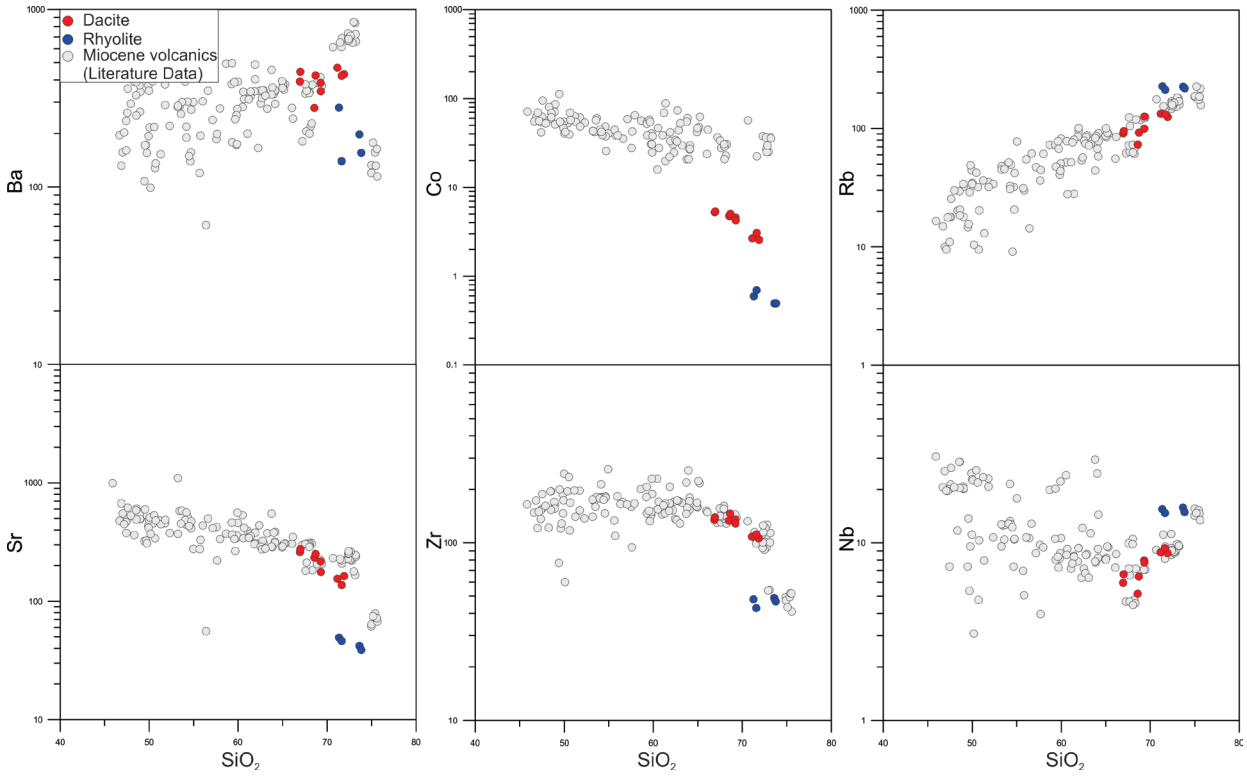

Fig. 7. Variation diagrams of SiO_2 (wt.%) versus trace elements (Harker 1909). The literature data is the same as in Fig. 5.

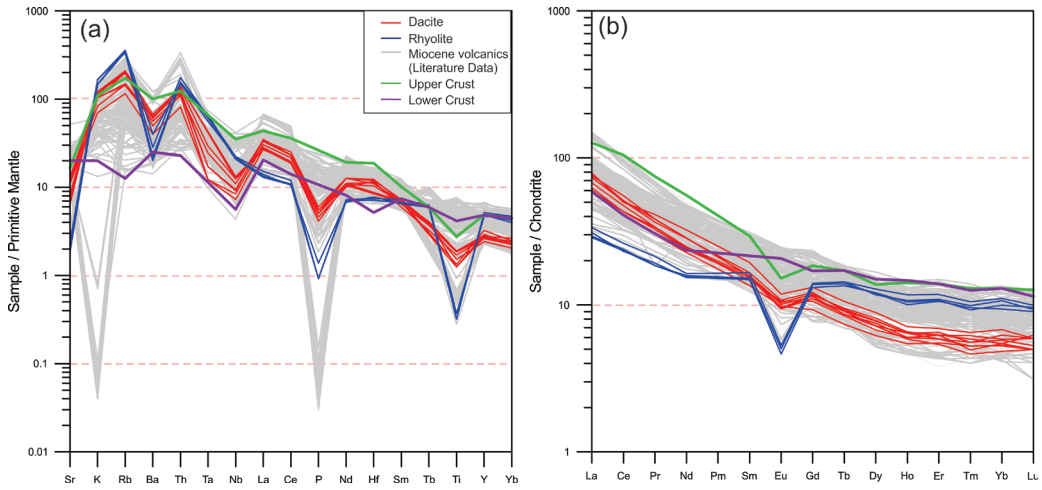

Fig. 8. a — Primitive mantle-normalised multi-element spidergram (Sun & McDonough 1989). **b** — Chondrite-normalised REE spidergram (Sun & McDonough 1989) for the lower Miocene felsic rocks in the Eskiköy–Doğanşehir (Malatya). Average Upper Crust and Lower crust values were taken from Sun & McDonough (1989). The literature data is the same as in Fig. 5.

rhyolitic lavas contain a distinct subduction component, but have been significantly modified by crustal melts (Haase et al. 2006).

On the chondrite normalised spidergram, the LREEs (La, Ce, Pr, Nd) exhibit more enrichment than HREEs (Er, Tm, Yb, Lu) and slightly negative Eu anomalies (Fig. 8b). Accordingly, it can be suggested that LREEs prefer the liquid phase during magmatic differentiation processes or partial melting (Rollinson 1993). The enrichment in LREEs can also occur with the contribution of the subducting slab to the magma source or with the effect of crustal contaminations (Hawkesworth et al. 1993). Negative Eu (Eu/Eu*=0.73–1.02) anomalies and upward concave pattern indicate significant plagioclase and amphibole fractionation of dacitic and rhyolitic lavas (Rollinson 1993; Fig. 8b).

Pb/Ce (0.07–3.7), La/Yb (4.16–23.17), Rb/Y (6.15–11.43), and Nb/Y (0.44–0.75) values can reveal fluid or melt-related enrichment, which is effective on mantle metasomatism.

The Pb/Ce versus La/Yb and Rb/Y versus Nb/Y diagrams (Fig. 13a, b) are significant in monitoring melt-related enrichment and fluid enrichment trends (Dhuime et al. 2009; Sahakyan et al. 2016). According to these diagrams, fluid-related enrichment is effective in the evolution of volcanic rocks. This suggests that fluids derived from the subducting oceanic crust are crucial in melting the mantle wedge (Scambelluri et al. 2007).

The Ta/Yb ratios of the dacite and rhyolites range between 0.44–1.28, and their Th/Yb ratios range between 5.71–10.73. The studied volcanics in the Th/Yb vs Ta/Yb diagram (Pearce 2008) present a parallel alignment to the mantle sequence but have high Th/Yb ratios (Fig. 14a). The enrichment in Th compared to the mid-ocean ridge basalt (MORB) mantle indicates the influence of subduction fluids (Weaver et al. 1986). This suggests that the volcanics did not undergo only a single fractional crystallisation differentiation in their development but were more likely exposed to various contamination processes. This diagram demonstrates that these rocks were probably derived from magmas evolved by fractional crystallisation processes and were enriched with subduction component plates (Pearce 1983). When all Miocene volcanic rocks in the region are plotted in this diagram, the primitive samples from the literature data (Arger et al. 2000; Yılmaz et al. 2007: Kürüm et al. 2008; Önal et al. 2008; Ekici et al. 2009; Ekici 2016; Kocaarslan & Ersoy 2018) plot in the mantle metasomatism field and gradually become richer in terms of the subduction zone component. At the same time, the dominant effect of fractional crystallisation and assimilation is quite evident in highly evolved dacitic and rhyolitic lavas.

The Nb/U ratios of the lower Miocene felsic rocks, which are markedly low, vary between 1.13–2.16. It is seen that the source magma is subjected to the upper crust (Fig. 14b). In Nb/La versus Ba/Rb diagram indicates that the studied rocks were affected by crustal assimilation (Fig. 14c). Some researchers suggest that the magmas derived from metasomatised mantle wedge by subduction zone melt have high Nb contents (7<Nb<20 ppm; e.g., Defant et al. 1992). The high Nb content of the rhyolites (14.8–15.9) supports the view that these rocks may have derived from a mantle source enriched by subduction-zone fluids. The high Nb values of the volcanic rocks indicate that these rocks assimilate a significant amount of crustal components. On the other hand, the average Nb value of the upper continental crust is 13.7±0.9 ppm (Plank &

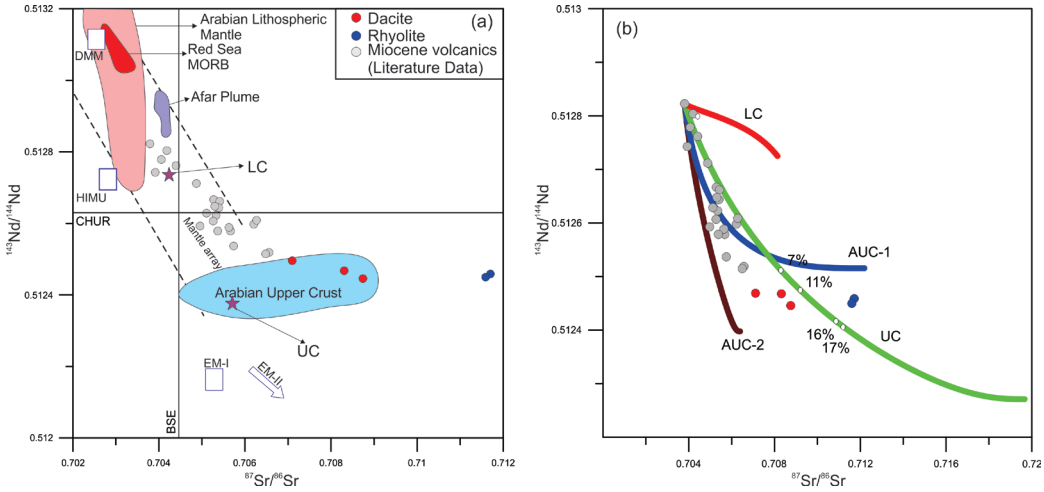

Fig. 9. a — $^{143}Nd/^{144}Nd$ versus ($^{87}Sr/^{86}Sr$) isotope correlation diagram of the lower Miocene felsic rocks in the Eskiköy–Doğanşehir (Malatya). BSE is the Bulk Silicate Earth; CHUR is the Chondritic Uniform Reservoir. DMM (Depleted MORB Mantle), HIMU=High μ (μ=$^{238}U/^{204}Pb$ ratio), EM-I (Enriched Mantle I), EM-II (Enriched Mantle II), Arabian Upper Crust, Arabian Lithospheric Mantle, Red Sea MORB, and Afar plume regions as in Ma et al. (2011). UC=Upper Crust and LC: Lower Crust (Taylor & McLennan 1985). **b** — EC-AFC modelling diagram (Bohrson & Spera 2001). The EC-AFC parameters for the standard upper-crustal (UC) case and standard lower-crustal (LC) case were taken from Bohrson & Spera (2001). For (AUC-1) Arabian upper crust muscovite schist case and (AUC-2) Arabian upper crust biotite granite–gneiss case were taken from Hegner & Pallister (1989). The literature data is the same as in Fig. 5.

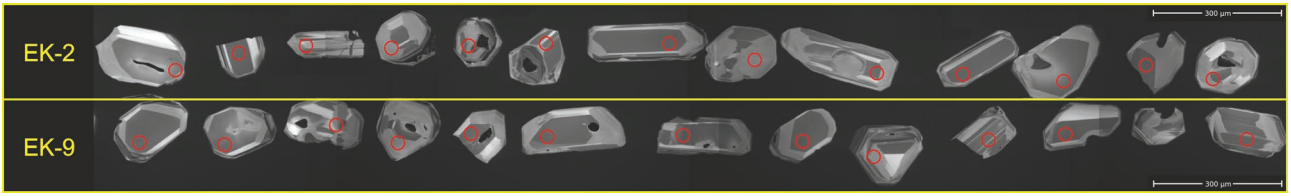

Fig. 10. Representative cathodoluminescence (CL) images of zircons from the lower Miocene felsic rocks, showing the locations of analysis points.

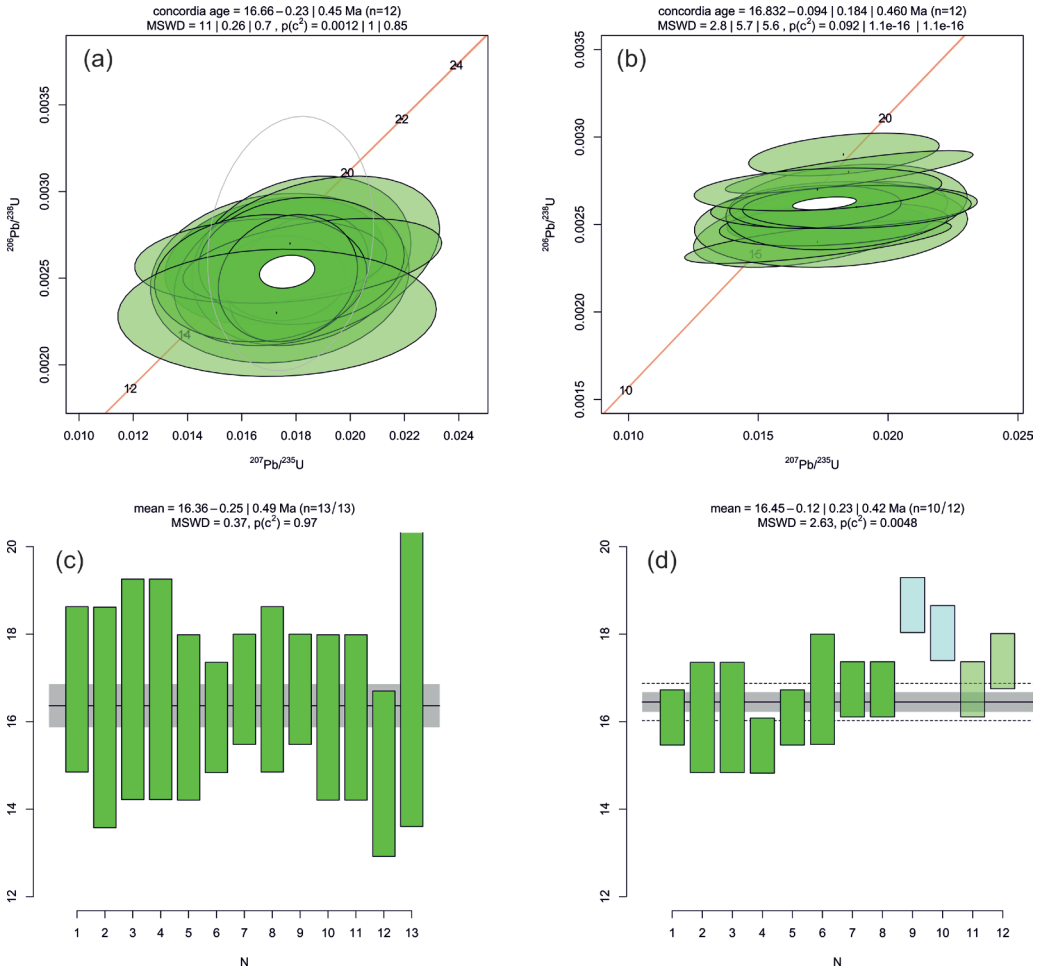

Fig. 11. Concordia (**a**, **b**) and weighted mean (**c**, **d**) diagrams for EK-2 and EK-9 samples from the lower Miocene felsic rocks.

Langmuir 1998). However, it is clear that rhyolitic lavas are highly evolved and mostly exhibit a behaviour close to crustal composition in other diagrams. Considering that all of the volcanic rocks in the region follow a distinct fractionation trend from mafic to felsic melts in the Harker diagrams, it can be concluded that dacitic and rhyolitic lavas were formed by high fractionation and crustal assimilation of mantle-derived mafic magmas.

The Sr–Nd isotopes of post-collisional Miocene volcanic rocks in the region were used to understand the magma evolution story and to determine the contribution of crustal melting to the evolution process. When the primary Sr–Nd isotope ratios are taken into account, it is seen that felsic volcanic rocks are mostly derived from crustal melts, while mafic volcanic rocks are derived from enriched mantle and/or lithospheric mantle sources. Based on the $^{143}Nd/^{144}Nd$ versus $^{87}Sr/Sr^{86}$ isotopic plot (Fig 9a), the lower Miocene felsic dikes show a trend toward the upper continental crust, implying that the crust contamination played a role in magma evolution (Beydokhti et al. 2015). This indicates that the possible upper crustal contribution was high, and the mantle contribution was low during the magma evolution. Dacites have εNd(t) values ranging from −3.12 to −3.60, and rhyolites have similar εNd(t) values from −3.48 to −3.66 (Suppl. Table S2). Rhyolites show greater depletion in Eu, Sr, P and Ti than dacites (Fig. 8a), suggesting that the rhyolitic magmas have undergone more fractionation of titanite (for Ti), apatite (for Sr), and K-feldspar (for Sr). These elemental and isotopic similarities may indicate that more upper crustal materials have generated dacitic and rhyolitic rocks (Zhao et al. 2017). Sr–Nd isotopic data suggest that the magmas were generated by partial melting of mixed sources comprising crust-derived and lithospheric mantle-derived melts. The geochemical and isotopic similarities between rhyolitic and dacitic rocks indicate rhyolites are more-fractionated products from the same batch melt as dacites. Low $^{143}Nd/^{144}Nd$ values indicate a hybrid composition in volcanics. This hybrid composition originates from a possible mixture of lithospheric mantle-derived magma and continental crust. The lower Miocene felsic rocks show negative εNd values ranging from −3.12 to −3.66, and based on these values, it is seen that the dacidic lavas are falling into the Arabian upper crustal field, while the rhyolitic lavas reflect the alteration effects with higher Sr isotope ratios. Moreover, the Nd (T_{DM}) model ages range from 1.05 to 1.13 Ga, and these values are consistent with the Precambrian basement rocks on Turkey, Iran and Arabian platform (for example, 1.0–1.8 Ga in

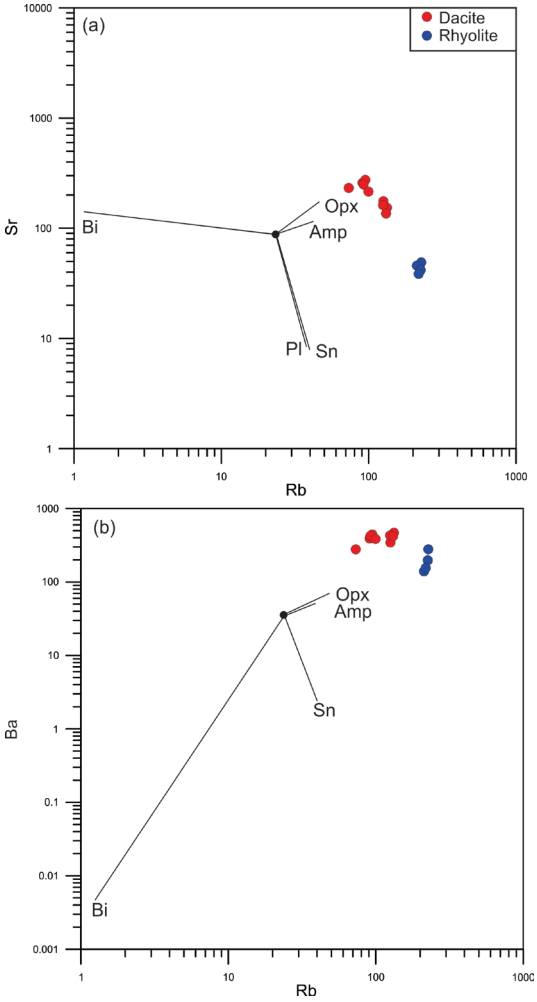

Fig. 12. a — Sr versus Rb log-log variation diagram, showing FC process. **b** — Ba versus Rb log-log variation diagram showing FC process. Each vector modelled and plotted on the diagrams represents up to 100 % crystallisation of mineral assemblages under the diagram according to Rayleigh crystallisation (FC: fractional crystallisation, Pl: plagioclase, Amp: amphibole, Opx: orthopyroxene, Bi: Biotite, Sn: sanidine) GERM Partition Coefficient (Kd) Database (https://earthref.org/).

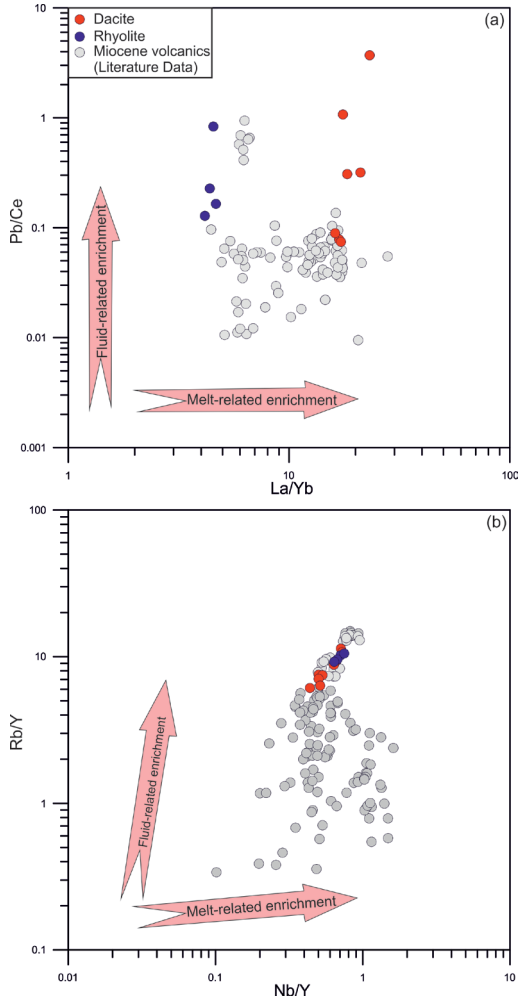

Fig. 13. a — Pb/Ce versus La/Yb. **b** — Rb/Y versus Nb/Y diagrams of the lower Miocene felsic rocks in the Eskiköy–Doğanşehir (Malatya). Vectors were taken from (Dhuime et al. 2009; Sahakyan et al. 2016). The literature data is the same as in Fig. 5.

the Menderes massif (Erkül & Erkül 2012); 1.13–2.16 Ga in the Bitlis massif (Ustaömer et al. 2012); in Derik volcanics 1.02–2.14 Ga (Gürsu et al. 2015), and Iran 1.35–1.65 Ga (Moghadam et al. 2015); 1.35–1.56 (Moradi et al. 2020)). When these data are evaluated together, it shows that the crustal melts derived from Precambrian basement rocks may have mixed with mafic melts, giving younger mantle Nd (T_{DM}) model ages (0.53 Ga, Suppl. Table S2).

Tectonic setting

The post-collisional convergence gave rise to crustal thickening and uplift of the East Anatolian region, as evidenced by the region-wide development of E–W trending folds and thrusts and conjugate strike-slip faults (Arger et al. 2000; Şengör et al. 2008). Consequently, the Miocene volcanics reached the surface along the N–S-oriented tensional structures. Parlak et al. (2001) stated that the settlement of mafic volcanism is derived from primary magma melts originating from the asthenosphere, and this magma is heavily exposed to crustal contamination. Keskin (2003) pointed out the slab steepening and break-off event model for magma genesis beneath a large subduction-accretion complex. This model holds a northward subducting oceanic slab beneath the large Eastern Anatolia accretionary prism that gets steepened and is eventually detached from the continental lithosphere. The Eastern Anatolian Accretionary Complex is a collision zone without a mantle plume complex, followed by a break-off (Şengör et al. 2003) at ca. 10–11 Ma. Calc-alkaline volcanism with a distinct subduction signature across Eastern Anatolia has been related to the first episode of slab-steepening event between ~15 and 10 Ma before slab break off at ~10 Ma

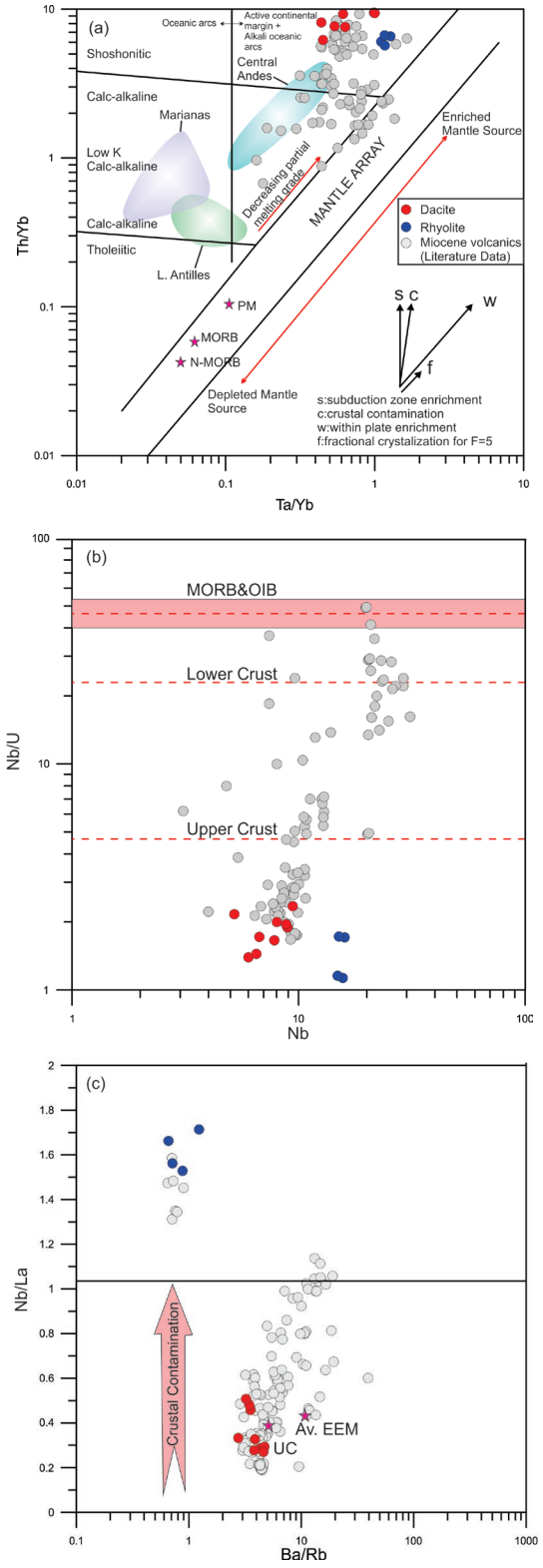

Fig. 14. a — Th/Yb versus Ta/Yb (Pearce 1983) diagrams of the lower Miocene felsic rocks in the Eskiköy–Doğanşehir (Malatya). The literature data is the same as in Fig. 5. **b** — Nb/U versus Nb diagram (Hofmann et al. 1986). **c** — Nb/La versus Ba/Rb diagram (Wang et al. 2004) of the lower Miocene felsic rocks in the Eskiköy–Doğanşehir (Malatya). UC (Average Upper Crust): McLennan (2001), av. EMM (average enriched mantle melts): Yang et al. (2004). The literature data is the same as in Fig. 5.

(Keskin 2003). Keskin (2007) mentioned that Eastern Anatolia is one of the best examples of an active continental collision zone in the world and suggested that the slab steepening and break-off model explains better than any other model for Eastern Anatolia, based on the southward younging age progression and changing lava geochemistry to the Na-alkaline compositions. Yılmaz et al. (2007) defined two-stage felsic volcanism in the western part of the SAOB. The authors emphasised that the first phases of magma developed by muscovite-dehydration melting, while the second phases indicate that these melt formed by water-saturated melting, and this volcanism occurred during both collisional and post-collisional periods in the late Oligocene to middle Miocene. Önal et al. (2008) reported that three different magmas effectively spatiotemporally formed Orduzu volcanics located east of the YVC. These are as follows: (i) calc-alkaline rhyolitic magma of crustal origin, (ii) calc-alkaline magma of lithospheric mantle origin, and (iii) moderately alkaline magma of lithospheric mantle origin. The authors proposed that the subduction signature in the enriched mantle source was derived from mantle metasomatism caused by the introduction of fluids sourced from an earlier supra-subduction zone. Kürüm et al. (2008) argued that the magmas parental to the middle Miocene YVC were derived from an enriched lithospheric mantle source metasomatised by fluids generated from earlier subduction post-collisional extensional geodynamic setting. Ekici et al. (2009) mentioned fractional crystallisation, magma mixing and crustal assimilation processes that effectively evolved collision-related volcanic rocks from Miocene YVC. Kürkçüoğlu et al. (2015) stated that the lithosphere plays an important role in the magma origin of the Pliocene basaltic rocks in their study carried out in the northeast of Sivas, and they marked that these rocks are derived from an asthenospheric (anorogenic) origin. Kocaarslan & Ersoy (2018) proposed that the Pliocene samples showing more primitive mantle characteristics outcropping in the Gürün and Kangal basins in the West-Southwest of the YVC exhibit intraplate (anorogenic) geochemical features. They also stated that the more evolved Miocene calc-alkaline samples are geochemically similar to subduction (orogenic) igneous rocks and can be affected by crustal contamination of primitive magmas with this anorogenic character. This hypothesis is an alternative to the general view, which assumes that the early-middle Miocene magmatic activity in the region is derived from a modified mantle source associated with the subduction of the Arabian Plate under the Anatolian Plate. Di Giuseppe et al. (2017) reported that the volcanism in the Elazığ, Tunceli and Bingöl provinces was formed through three stages of activity; (i) the lower-middle Miocene (16.3–15.5 Ma) calc-alkaline basaltic trachyandesite to dacites in the Pertek and Mazgirt regions, (ii) the upper Miocene (11.4–11.0 Ma) transitional basalts in the Tunceli region, (iii) Plio-Pleistocene Na-alkali basalts (4.1 Ma–1.7 Ma) in Karakoçan region and Elazığ region. They concluded that the early-middle Miocene magmas in a convergent setting indicate derivation from mantle sources modified by subduction signatures. In contrast, the upper

Miocene transitional basalts are associated with the change from compressional to strike-slip tectonic regimes. During the development of tectonism, passive upwelling of the local sub-slab mantle led to the starting of Na-alkali basaltic activity. Karaoğlu et al. (2020) stated that the Karlıova–Varto volcanic activity developed in the triple junction area in Eastern Anatolia, ranging in compositions from basalt to rhyolite during Miocene to Quaternary. The authors indicated that subduction-related signatures mainly exhibit volcanic rocks. Most of the primary magma characteristics are severely exposed to crustal assimilation and fractionation processes after developing tectonic systems in the region. Lin et al. (2020) stated that the age data indicate a diachronous onset of volcanism that began ~17 Ma in Southeast Anatolia and propagated northward from ~11 to 9 Ma toward Northeast Anatolia and Iran. According to the authors, the volcanic rocks were formed during the initial stage of post-collisional magmatism in the Caucasus-Iran-Anatolia province. Kürüm et al. (2021) suggested that the early to middle Miocene Pertek adakitic volcanism was triggered by collision and slab break-off-induced asthenospheric mantle flows in Eastern Anatolia.

The subduction-related geochemical signatures were probably inherited from the mantle lithosphere enriched by slab-derived fluids released during the northward subduction of the Afro-Arabian plate beneath Anatolia (Pearce et al. 1990). During this magmatic episode, slab-derived fluids significantly impacted the parental magma. In the early Miocene, post-collisional Neogene volcanism produced calc-alkaline to high K calc-alkaline volcanic rocks in this region. Post-collisional Neogene–Quaternary magmatism was most likely caused by lithospheric delamination and slab tearing/rollback in the Eastern and Central Anatolia volcanic provinces, respectively (Schleiffarth et al. 2018). Slab break-off will open a slab window and trigger partial melting of differing magma source regions, producing post-collisional magmatism (Keskin 2003, 2007). Our findings and the literature data of this period are evaluated together and indicate that the lower Miocene felsic rocks record an evolution from a post-collisional tectonic setting.

Conclusions

- Lower Miocene felsic rocks are represented by dacitic to rhyolitic rocks. The main mineral assemblage of dacites comprises plagioclase, quartz, biotite and amphibole, while the rhyolites comprise quartz, sanidine, plagioclase, biotite and amphibole.
- The concordia ages of the Eskiköy–Doğanşehir volcanics are 16.66±0.23 and 16.83±0.094 Ma (early Miocene), and these ages are an important contribution to understanding the onset of post-collisional magmatism in the region.
- The Energy-Constrained Assimilation-Fractional Crystallisation (EC-AFC) model suggests significant upper-crust assimilation during the evolution of the volcanics.
- Geochemical and Sr–Nd isotopic data indicate that the lower Miocene felsic rocks may have originated from mixing crust-derived melts and lithospheric mantle-derived mafic melts.
- The geochemistry, geochronology and regional geology suggest that the parental magma of the lower Miocene volcanics were derived from a lithospheric mantle source that was metasomatised by slab-derived fluids and magma generated by fractional crystallisation assimilation events in a post-collisional tectonic setting.

Acknowledgements: In this study, some geochemical data were reproduced from the second author's PhD thesis. This research was supported by Fırat University Scientific Research Project Management Unit (Project No: MF 16.63 and MF 22.18). The authors would also like to thank the editors and anonymous reviewers for their constructive comments and suggestions, which improved the manuscript.

References

Agostini S., Savaşçin, M.Y., Di Giuseppe P., Di Stefano Flavio., Karaoğlu Ö., Lustrino, M., Manetti, Piero., Ersoy, Y., Kürüm, S. & Öztufekçi Önal A. 2019: Neogene volcanism in Elazığ-Tunceli area (eastern Anatolia): geochronological and petrological constraints. *Italian Journal of Geosciences* 138, 435–455. https://doi.org/10.3301/IJG.2019.18

Arger J., Mitchell J. & Westaway R.W.C. 2000: Neogene and Quaternary volcanism of southeastern Turkey. In: Bozkurt E., Winchester J. & Piper J.A. (Ed.): Tectonics and magmatism in Turkey and the surrounding area. *Geological Society, London, Special Publications* 173, 459–487. https://doi.org/10.1144/GSL.SP.2000.173.01.22

Asan K. 2020: Whole-rock elemental and Sr-Nd isotope geochemistry and petrogenesis of the Miocene Elmadağ Volcanic Complex, Central Anatolia (Ankara, Turkey). *Geosciences* 10, 348. https://doi.org/10.3390/geosciences10090348

Beyarslan M., Okta E. & Ertürk M.A. 2018: Kale (Malatya) İlçesi Çevresindeki Geç Kretase Yaşlı Yay Magmatitlerinin Jeokimyasal Özellikleri. *Erzincan University Journal of Science and Technology* 11, 191–206. https://doi.org/10.18185/erzifbed.405603

Beyarslan M., Ertürk M.A., Rizeli M.E. & Sar A. 2022: Petrogenesis and Tectonic Setting of the Quaternary Mafic Alkaline Harput Volcanic Rocks Along with the East Anatolian Fault System, Southeastern Anatolia Orogenic Belt (Elazığ). *ECJSE* 9, 171–188. https://doi.org/10.31202/ecjse.955277

Beydokhti R.M., Karimpour M.H., Mazaheri, S.A. Santos J.F. & Klötzli U. 2015: U–Pb zircon geochronology, Sr–Nd geochemistry, petrogenesis and tectonic setting of Mahoor granitoid rocks (Lut Block, Eastern Iran), *Journal of Asian Earth Sciences* 111, 92–205. https://doi.org/10.1016/j.jseaes.2015.07.028

Bohrson W.A. & Spera F. 2001: Energy-Constrained Open-System Magmatic Processes II: Application of Energy-Constrained Assimilation-Fractional Crystallization (EC-AFC) Model to Magmatic Systems. *Journal of Petrology* 42, 1019–1041. https://doi.org/10.1093/petrology/42.5.1019

Caran Ş. & Polat S. 2022: Petrology of Mt. Kıra continental alkali lavas with arc-like signature, Batman, SE Anatolia, Turkey: Evidence for mafic juvenile lower crust assimilated intraplate basalts in the collision- and mantle flow-driven geodynamic setting of Arabian Foreland. *Lithos* 106645, 416–417. https://doi.org/10.1016/j.lithos.2022.106645

Defant M.J., Jackson T.E., Drummond M.S., De Boer J.Z., Bellon H., Feigenson M.D., Maury R.C. & Stewart R.H. 1992: The geochemistry of young volcanism throughout western Panama and southeastern Costa Rica: an overview. *Journal of the Geological Society* 149, 569–579. https://doi.org/10.1144/gsjgs.149.4.0569

Dhuime B., Bosch D., Garrido C.J., Bodinier J.L., Bruguier O., Hussain S.S. & Dawood H. 2009: Geochemical Architecture of the Lower- to Middle-crustal Section of a Paleo-island Arc (Kohistan Complex, Jijal-Kamila Area, Northern Pakistan): Implications for the Evolution of an Oceanic Subduction Zone. *Journal of Petrology* 50, 531–569. https://doi.org/10.1093/petrology/egp010

Di Giuseppe P., Agostini S., Lustrino M., Karaoğlu Ö., Savaşçın M.Y., Manetti P. & Ersoy E.Y. 2017: Compression to strike-slip tectonics shift as revealed by Miocene-Pleistocene volcanism west of the Karlıova triple junction (East Anatolia). *Journal of Petrology* 58, 2055–2087. https://doi.org/10.1093/petrology/egx082

Ekici T. 2016: Collision-related slab break-off volcanism in the Eastern Anatolia, Kepez volcanic complex (TURKEY). *Geodinamica Acta* 28, 223–239. https://doi.org/10.1080/09853111.2015.1121796

Ekici T., Alpaslan M., Parlak O. & Temel A. 2007: Geochemistry of the Pliocene basalts erupted along the Malatya-Ovacık fault zone (MOFZ), eastern Anatolia, Turkey: implications for source characteristics and partial melting processes. *Geochemistry* 67, 201–212. https://doi.org/10.1016/j.chemer.2006.01.007

Ekici T., Alpaslan M., Parlak O. & Uçurum A. 2009: Geochemistry of the Middle Miocene collision-related Yamadağı (Eastern Anatolia) calc-alkaline Volcanics, Turkey. *Turkish Journal of Earth Sciences* 18, 511–528. https://doi.org/10.3906/yer-0712-1

Elmas A. & Yılmaz Y. 2003: Development of an oblique subduction zone tectonic evolution of the Tethys suture zone in Southeast Turkey. *International Geology Review* 45, 827–840. https://doi.org/10.2747/0020-6814.45.9.827

Erkül S.T. & Erkül F. 2012: Petrogenesis of Pan-African metagranitoids in the central Menderes Massif, Turkey: Contribution of geochemical and Sr–Nd isotopic data to the study of source rock characteristics. In: 12th International Multidisciplinary Scientific Geo Conference Proceedings 1, Albena, Bulgaria, 241–248.

Ertürk M.A., Beyarslan M., Chung S.-L. & Lin T.-H. 2018: Eocene magmatism (Maden Complex) in the Southeast Anatolian Orogenic Belt: Magma genesis and tectonic implications. *Geoscience Frontiers* 9, 1829–1847. https://doi.org/10.1016/j.gsf.2017.09.008

Ertürk M.A., Beyarslan M. & Sar A. 2017: In the Case of Maden Complex, Geochemical Constraints on the Origin and Tectonic Implication of Eocene Magmatism in SE Turkey. *Journal of Tethys* 5, 240–263.

Ertürk M.A., Sar A. & Rizeli M.E. 2022: Petrology, zircon U–Pb geochronology and tectonic implications of the A_1-type intrusions: Keban region, eastern Turkey. *Geochemistry* 82, 125882. https://doi.org/10.1016/j.chemer.2022.125882

Faure G. & Mensing T.M. 2005: Isotopes: Principles and Applications, 3rd ed. *John Wiley and Sons*, USA, 1–897.

Grimes C.B., Wooden J.L., Cheadle M.J. & John B.E. 2015: Fingerprinting tectonomagmatic provenance using trace elements in igneous zircon. *Contributions to Mineralogy and Petrology* 170, 1–26. https://doi.org/10.1007/s00410-015-1199-3

Gürsoy H., Tatar O., Piper J.D.A., Koçbulut F., Akpınar Z., Huang B. & Mesci B.L. 2011: Palaeomagnetic study of the Kepezdağ and Yamadağ volcanic complexes, central Turkey: Neogene tectonic escape and block definition in the central-east Anatolides. *Journal of Geodynamics* 51, 308–326. https://doi.org/10.1016/j.jog.2010.07.004

Haase K.M., Stroncik N., Garbe-Schönberg D. & Stoffers P. 2006. Formation of island arc dacite magmas by extreme crystal fractionation: An example from Brothers Seamount, Kermadec island arc (SW Pacific). *Journal of Volcanology and Geothermal Research* 152, 316–330. https://doi.org/10.1016/j.jvolgeores.2005.10.010

Harker A. 1909: The Natural History of Igneous Rocks. *Metheuen*, London, 1–384.

Hastie A.R., Kerr A.C., Pearce J.A. & Mitchell S.F. 2007: Classification of altered volcanic island arc rocks using immobile trace elements: development of the Th–Co discrimination diagram. *Journal of Petrology* 48, 2341–2357. https://doi.org/10.1093/petrology/egm062

Hawkesworth C.J., Gallagher K., Herot J.M. & McDermott F. 1993: Mantle and slab contributions in arc magmas. *Annual Review of Earth and Planetary Sciences* 21,175–204. https://doi.org/10.1146/annurev.ea.21.050193.001135

Hegner E. & Pallister J.S. 1989: Pb, Sr, and Nd isotopic characteristics of Tertiary Red Sea Rift volcanics from the central Saudi Arabian coastal plain. *Journal of Geophysical Research* 94, 7749–7755.

Hofmann A.W., Jochum K.P., Seufer M. & White W.M. 1986: Nb and Pb in oceanic basalts: new constraints on mantle evolution. *Earth and Planetary Science Letters* 79, 33–45.

Kara H. & Bal Akkoca D. 2021: Origin of Barite Mineralization in the Doğanşehir (Malatya): Trace and Rare Earth Element, Isotope and Fluid Inclusion Evidence. *ECJSE* 8, 1035−1050. https://doi.org/10.31202/ecjse.910527

Kara H. & Sağıroğlu S. 2018: Keban ve Malatya Metamortfitleri'ne ait organik madde içeren kayaçların iz ve nadir toprak element jeokimyası. *Fırat Üniversitesi Fen Bilimleri Dergisi* 30, 1–10.

Karaoğlan F., Parlak. O., Hejl. E., Neubauer, F. & Klötzli U. 2016: The temporal evolution of the Active Margin along the Southeast Anatolian Orogenic Belt (SE Turkey): Evidence from U–Pb, Ar–Ar and Fission Track Chronology. *Gondwana Research* 33, 190–208. https://doi.org/10.1016/j.gr.2015.12.011

Karaoğlan F., Parlak O., Robertson A., Thöni M., Klötzli U., Koller F. & Okay A.İ. 2013: Evidence of Eocene high-temperature/high-pressure metamorphism of ophiolitic rocks and granitoid intrusion related to Neo-Tethyan subduction processes (Doğanşehir area, SE Anatolia). *Geological Society, London, Special Publications* 372, 249–272. https://doi.org/10.1144/SP372.21

Karaoğlu Ö., Gülmez F., Göçmengil G., Lustrino M., Di Giuseppe P., Manetti P., Savaşçın M.Y. & Agostini S. 2020: Petrological evolution of Karlıova-Varto volcanism (Eastern Turkey): magma genesis in a transtensional triple-junction tectonic setting. *Lithos* 364–365, 105524. https://doi.org/10.1016/j.lithos.2020.105524

Gürsu S., Möller A., Göncüoglu M.C., Köksal S., Demircan H., Toksoy-Köksal F., Kozlu H. & Sunal G. 2015: Neoproterozoic continental arc volcanism at the northern edge of the Arabian Plate, SE Turkey. *Precambrian Research* 258, 208–233. https://doi.org/10.1016/j.precamres.2014.12.017

Keskin M. 2003: Magma generation by slab steepening and break-off beneath a subduction accretion complex: an alternative model for collision related volcanism in Eastern Anatolia, Turkey. *Geophysical Research Letters* 30, 8046–8050. https://doi.org/10.1029/2003GL018019

Keskin M. 2007: Eastern Anatolia: a hot spot in a collision zone without a mantle plume. In: Foulger G.R. & Jurdy D.M. (eds.): Plates, Plumes and Planetary Processes. *Geological Society of America Bulletin* 43, 693–722. https://doi.org/10.1130/2007.2430(32)

Kocaarslan A. & Ersoy E.Y. 2018: Petrologic evolution of Miocene–Pliocene mafic volcanism in the Kangal and Gürün basins (Sivas–Malatya), central east Anatolia: Evidence for Miocene anorogenic magmas contaminated by continental crust. *Lithos* 310, 392–408. https://doi.org/10.1016/j.lithos.2018.04.021

Köksal S. 2019: The Upper Cretaceous intrusive rocks with extensive crustal contribution in Hacımahmutuşagı Area (Aksaray/Turkey). *Geologica Carpathica* 70, 261–276. https://doi.org/10.2478/geoca-2019-0015

Kürkçüoğlu B., Pickard M., Şen P., Hanan B.B., Sayit K., Plummer C., Sen E., Yurur T. & Furman T. 2015: Geochemistry of mafic lavas from Sivas, Turkey and the evolution of Anatolian lithosphere. *Lithos* 232, 229–241. https://doi.org/10.1016/j.lithos.2015.07.006

Kürüm S., Önal A., Boztuğ D, Spell T. & Arslan M. 2008: $^{40}Ar/^{39}Ar$ age and geochemistry of the post-collisional Miocene Yamadağ volcanics in the Arapkir area (Malatya Province), eastern Anatolia, Turkey. *Journal of Asian Earth Sciences* 33, 229–251. https://doi.org/10.1016/j.jseaes.2007.12.001

Kürüm S., Çoban H. & Aydın P. 2021: Generation of collision-induced Early to Middle Miocene adakitic magmas in Pertek (Tunceli) area from Eastern Anatolia postsubductional setting, Turkey. *Turkish Journal of Earth Sciences* 30, 948–972. https://doi.org/10.3906/yer-2104-16

Le Bas M.J., Le Maitre R.W., Streckeisen A. & Zanettin B. 1986: A chemical classification of volcanic rocks based on the total alkali-silica diagram. *Journal of Petrology* 27, 745–750. https://doi.org/10.1093/petrology/27.3.745

Leo G.W., Marvin R.F. & Mehnert H.H. 1974: Geologic framework of the Kuluncak–Sofular area, east-central Turkey, and K–Ar ages of igneous rocks. *Geological Society of America Bulletin* 85, 1785–1788.

Lin Y.-C., Chung S.-L., Bingöl A.F., Yang L., Okrostsvaridze A., Pang K.-N., Lee H.-Y. & Lin T.-H. 2020: Diachronous initiation of post-collisional magmatism in the Arabia-Eurasia collision zone. *Lithos* 105394, 356–357.

Lugmair G.W. & Marti K. 1978: Lunar initial $^{143}Nd/^{144}Nd$: differential evolution of the lunar crust and mantle. *Earth and Planetary Science Letters* 39, 349–357. https://doi.org/10.1016/0012-821X(78)90021-3

Ma G.S.-K., Malpas J., Xenophontos C. & Chan G.H.-N. 2011: Petrogenesis of Latest Miocene-Quaternary Continental Intraplate Volcanism along the Northern Dead Sea Fault System (Al Ghab-Homs Volcanic Field), Western Syria: Evidence for Lithosphere–Asthenosphere Interaction. *Journal of Petrology* 52, 401–430. https://doi.org/10.1093/petrology/egq085

McDonough W.F. 1991: Geochemical and isotopic systematics of continental lithospheric mantle. In: Meyer H.O.A. & Leonardos O.H. (eds.): Kimberlites, Related Rock and Mantle Xenoliths. *Companhian de Pequisa de Recursos Minerais* 1, Rio de Janeiro, 478–485.

McLennan S.M. 1989: Rare Earth Elements in Sedimentary Rocks: Influence of Provenance and Sedimentary Process. *Review of Mineralogy* 21, 169–200.

McLennan S.M. 2001: Relationships between the trace element composition of sedimentary rocks and upper continental crust. *Geochemistry Geophysics Geosystems* 2, 2000GC00109.

Menzies M.A. 1983: Mantle ultramafic xenoliths in alkaline magmas: evidence for mantle heterogeneity modified by magmatic activity. In: Hawkesworth C.J. & Norry M.J. (eds.): Continental Basalts and Mantle Xenoliths. *Shiva Publishing*, Nantwich, 92–110.

Middlemost E.A.K. 1994: Naming materials in the magma/igneous rock system. *Earth Science Reviews* 37, 215–224. https://doi.org/10.1016/0012-8252(94)90029-9

Moghadam H.S., Khademöi M., Hu Z.C., Stern R.J., Santos J.F. & Wu Y.B. 2015: Cadomian (Ediacaran–Cambrian) Arc Magmatism in the Chah-Jam-Biairmand metamorphic complex (Iran): Magmatism along the northern active margin of Gondwana: *Gondwana Research* 27, 439–452.

Moradi A., Shabanian N., Davoudian A.R., Azizi H., Santos J.F. & Asahara Y. 2020: Geochronology and petrogenesis of the Late Neoproterozoic granitic gneisses of Golpayegan metamorphic complex: a new respect for Cadomian crust in the Sanandaj–Sirjan zone, Iran. *International Geology Review* 64, 1450–1473. https://doi.org/10.1080/00206814.2020.1821251

M.T.A. 2013: Magmatic Rocks Map of Turkey. *General Directorate of Mineral Research and Explorations*, Ankara, Turkey.

Nurlu N., Parlak O., Robertson A.H.F. & Quadt A. 2016: Implications of Late Cretaceous U–Pb zircon ages of granitic intrusions cutting ophiolitic and volcanogenic rocks for the assembly of the Tauride allochthon in SE Anatolia (Helete area, Kahramanmaras¸ region, SE Turkey). *International Journal of Earth Sciences* 105, 283–314. https://doi.org/10.1007/s00531-015-1211-1

Nurlu N., Köksal S. & Kohút M. 2022: Late Cretaceous volcanic arc magmatism in southeast Anatolian Orogenic Belt: Constraints from whole-rock, mineral chemistry, Sr–Nd isotopes and U–Pb zircon ages of the Baskil Intrusive Complex (Malatya, Turkey). *Geological Journal* 57, 3048–3073. https://doi.org/10.1002/gj.4460

Okay A.I. & Tüysüz O. 1999: Tethyan sutures of northern Turkey. *Geological Society, London, Special Publications* 156, 475–515. https://doi.org/10.1144/GSL.SP.1999.156.01.22

Önal A. 1995: Polat-Beğre (Doğanşehir) çevresindeki magmatik kayaçların petrografik ve petrolojik özellikleri. *PhD Thesis, Fırat Üniv Fen Bilim Enst Elazığ*, Türkiye.

Önal A. & Altunbey M. 1999: Dedeyazı-Çavuşlu (Doğanşehir–Malatya) yöresindeki skarn oluşumlar ve ilişkili demir cevherleşmeleri. *Türkiye Jeoloji Bülteni* 1, 15–27.

Önal A. & Beyarslan M. 2001: Doğanşehir (Malatya) civarındaki ofiyolitik kayaçların jeolojik ve petrografik özellikleri. *Selçuk Üniv. Müh-Mimarlık Fak Dergisi* 16, 66–75.

Önal A., Boztuğ D., Arslan M., Spell T.L. & Kürüm S. 2008: Petrology and $^{40}Ar–^{39}Ar$ Age of the Bimodal Orduzu Volcanics (Malatya) from the Western end of the Eastern Anatolian Neogene Volcanism, Turkey. *Turkish Journal of Earth Sciences* 17, 85–109.

Özdemir Y., Oyan V. & Jourdan F. 2022: Petrogenesis of Middle Miocene to Early Quaternary basalts from the Karayazı–Göksu plateau (Eastern Anatolia, Turkey): Implication for the role of pyroxenite and lithospheric thickness. *Lithos* 106671, 416–417. https://doi.org/10.1016/j.lithos.2022.106671

Parlak O., Delaloye M., Demirkol C. & Ünlügenç U.C. 2001: Geochemistry of Pliocene/Pleistocene basalts along the Central Anatolian Fault Zone (CAFZ), Turkey. *Geodinamica Acta* 14, 159–167. https://doi.org/10.1016/S0985-3111(00)01062-7

Parlak O., Karaoglan F., Rizaoglu T., Nurlu N., Bagci U., Höck V., Öztüfekçi-Önal A., Kürüm S. & Topak Y. 2013: Petrology of the Ispendere (Malatya) ophiolite from the Southeast Anatolia: implications for the Late Mesozoic evolution of the southern Neotethyan Ocean. *Geological Society Special Publication* 372, 219–247. https://doi.org/10.1144/SP372.11

Pearce J.A., Bender J.F., De Long S.E., Kidd W.S.F., Low P.J., Güner Y., Şaroğlu F., Yılmaz Y., Moorbath S. & Mitchell J.G. 1990: Genesis of collision volcanism in Eastern Anatolia, Turkey. *Journal of Volcanology and Geothermal Research* 44, 189–229. https://doi.org/10.1016/0377-0273(90)90018-B

Pearce J.A. 1983: The role of sub-continental lithosphere in magma genesis at destructive plate margins. In: Hawkesworth C.J. & Norry M.J. (eds.): Continental Basalts and Mantle Xenoliths. *Sheva*, 230–249.

Pearce J.A. 2008: Geochemical fingerprinting of oceanic basalts with applications to ophiolite classification and the search for Archean oceanic crust. *Lithos* 100, 14–48. https://doi.org/10.1016/j.lithos.2007.06.016

Peccerillo A. & Taylor S.R. 1976: Geochemistry of Eocene calcalkaline volcanic rocks from the Kastasmonu area, north Turkey. *Contributions to Mineralogy and Petrology* 58, 63–81.

Plank T. & Langmuir C.H. 1998: The chemical composition of subducting sediment and its consequences for the crust and mantle. *Chemical Geology* 145, 325–394. https://doi.org/10.1016/S0009-2541(97)00150-2

Platzman E.S., Tapirdamaz C. & Sanver M. 1998: Neogene anticlockwise rotation of Central Anatolia (Turkey): Preliminary palaeomagnetic and geochronological results. *Tectonophysics* 299, 175–189. https://doi.org/10.1016/S0040-1951(98)00204-2

Rabayrol F., Hart C.J.R. & Thorkelson D.J. 2019: Temporal, spatial and geochemical evolution of late Cenozoic post-subduction magmatism in central and eastern Anatolia, Turkey. *Lithos* 336–337, 67–96. https://doi.org/10.1016/J. LITHOS.2019.03.022

Rizeli M.E., Beyarslan M., Wang K.-L. & Bingöl A.F. 2016: Mineral chemistry and petrology of mantle peridotites from the Guleman ophiolite (SE Anatolia, Turkey): Evidence of a forearc setting.

Journal of African Earth Sciences 123, 392–402. https://doi.org/10.1016/j.jafrearsci.2016.08.013

Rizeli M.E., Sar A. & Ertürk M.A. 2021: Petrographic and Geochemical Properties of the Keban Magmatic Rocks (Keban-Elazığ). *Mühendislik Bilimleri ve Araştırmaları Dergisi* 3, 69–80. https://doi.org/10.46387/bjesr.883632

Rollinson H. 1993: Using Geochemical Data: Evaluation, Presentation, Interpretation. *John Wiley & Sons*, New York, 1–352.

Sağıroğlu A., Kara H. & Kürüm S. 2013: Mineralogy and geochemistry of the hematite muscovite schists of Malatya, Turkey: Could it be the first known banded iron formation (BIF) in the Taurids And Anatolia? *Carpathian Journal of Earth And Environmental Sciences* 8, 49–58.

Sahakyan L., Bosch D., Sosson M., Avagyan A., Galoyan G.H., Rolland Y., Bruguier O., Stepanyan Z.H., Galland B. & Vardanyan S. 2016: Geochemistry of the Eocene magmatic rocks from the Lesser Caucasus area (Armenia): evidence of a subduction geodynamic environment. *Geological Society, London, Special Publications* 428, 73. https://doi.org/10.1144/SP428.12

Sar A., Ertürk M.A. & Rizeli M.E. 2019: Genesis of Late Cretaceous intra-oceanic arc intrusions in the Pertek area of Tunceli Province, eastern Turkey, and implications for the geodynamic evolution of the southern Neo-Tethys: Results of zircon U–Pb geochronology and geochemical and Sr-Nd isotopic analyses. *Lithos* 350–351, 105263. https://doi.org/10.1016/j.lithos.2019.105263

Sar A., Rizeli M.E. & Ertürk M.A. 2022: Petrographic and Geochemical Characteristics of the Rocks Belonging to the Elazig Magmatic Complex in the Geçityaka region (Tunceli). *ECJSE* 9, 680–694. https://doi.org/10.31202/ecjse.993333

Scambelluri M., Malaspina N. & Hermann J. 2007: Subduction fluids and their interaction with the mantle wedge: A perspective from the study of high-pressure ultramafic rocks. *Periodico di Mineralogia* 76, 253–265.

Schleiffarth W.K., Darin M.H., Reid M.R. & Umhoefer P.J. 2018: Dynamics of episodic Late Cretaceous–Cenozoic magmatism across Central to Eastern Anatolia. *Geosphere* 14, 1990–2008. https://doi.org/10.1130/GES01647.1

Şengör A.M.C., Özeren S., Genç T. & Zor E. 2003: East Anatolian high plateau as a mantle-supported, north-south shortened domal structure. *Geophysical Research Letters* 30, 8045. https://doi.org/10.1029/2003GL017858

Şengör A.M.C., Özeren M.S., Keskin M., Sakınç M., Özbakır A.D. & Kayan I. 2008: Eastern Turkish high plateau as a small Turkic-type orogen: Implications for post-collisional crust-forming processes in Turkic-type orogens. *Earth Science Reviews* 90, 1–48. https://doi.org/10.1016/j.earscirev.2008.05.002

Şengör A.M.C. & Yılmaz Y. 1981: Tethyan evolution of Turkey: a plate tectonic approach. *Tectonophysics* 75, 181–241.

Steiger R.H. & Jäger E. 1977: Subcommission on geochronology: convention on the use of decay constants in geo- and cosmochronology. *Earth and Planetary Science Letters* 36, 359–362. https://doi.org/10.1016/0012-821X(77)90060-7

Sun S.S. & McDonough W.F. 1989: Chemical and isotopic systematics of oceanic basalts: implications for mantle composition and processes, In: Saunders A.D. & Norry M.J. (eds.): Magmatism in Ocean Basins. *Geological Society, London, Special Publications* 42, 313–345.

Ural M., Arslan M., Göncüoğlu U.K. & Kürüm S. 2015: Late Cretaceous arc and back-arc formation within the Southern Neotethys: whole-rock, trace element and Sr-Nd-Pb isotopic data from basaltic rocks of the Yüksekova Complex (Malatya–Elazığ, SE Turkey). *Ofioliti* 40, 57–72. https://doi.org/10.4454/ofioliti.v40i1.435

Ural M., Sayıt K., Koralay O.E. & Göncüoğlu M.C. 2021: Geochemistry and Zircon U-Pb Dates of Felsic-Intermediate Members of the Late Cretaceous Yüksekova Arc Basin: Constraints on the Evolution of the Bitlis–Zagros Branch of Neotethys (Elazığ, E Turkey). *Acta Geologica Sinica – English Edition* 95, 1199–1216. https://doi.org/10.1111/1755-6724.14694

Ural M., Sayıt K. & Tekin U.K. 2022: Whole-Rock and Nd–Pb isotope geochemistry and radiolarian ages of the volcanics from the Yüksekova Complex (Maden Area, Elazığ, E Turkey): Implications for a Late Cretaceous (Santonian-Campanian) Back-Arc basin in the southern Neotethys. *Ofioliti* 47, 65–83. https://doi.org/10.4454/ofioliti.v47i1.552

Ustaömer P.A., Ustaömer T., Gerdes A., Robertson A.H.F. & Collins A.S. 2012: Evidence of Precambrian sedimentation/magmatism and Cambrian metamorphism in the Bitlis Massif, SE Turkey utilising whole-rock geochemistry and U–Pb LA-ICP-MS zircon dating. *Gondwana Research* 21, 1001–1018. https://doi.org/10.1016/j.gr.2011.07.012

Taylor S.R. & McLennan S.M. 1985: The Continental Crust: Its Composition and Evolution. *Blackwell*, 1–312.

Topuz G., Candan O., Zack T. & Yılmaz A. 2017: East Anatolian plateau constructed over a continental basement: no evidence for the east Anatolian accretionary complex. *Geology* 45, 791–794. https://doi.org/10.1130/G39111.1

Topuz G., Candan O., Zack T., Chen F. & Qiu-Li L. 2019: Origin and significance of Early Miocene high-potassium I-type granite plutonism in the East Anatolian plateau (the Taşlıçay intrusion). *Lithos* 105210, 348–349. https://doi.org/10.1016/j.lithos.2019.105210

Wang K.L., Chung S., O'Reilly S.Y., Sun S., Shinjo R. & Chen C. 2004: Geochemical constraints for the genesis of post-collisional magmatism and the geodynamic evolution of the Northern Taiwan region. *Journal of Petrology* 45, 975–1011. https://doi.org/10.1093/petrology/egh001

Weaver B.L., Wood D.A., Tarney J. & Joron J.L. 1986: Role of subducted sediment in the genesis of ocean-island basalts: Geochemical evidence from South Atlantic Ocean islands. *Geology* 14, 275–278.

Wilson M. 1989: Igneous Petrogenesis, in a Global Tectonic Approach. *Chapman and Hall*, London, 1–466.

Yang J.H., Wu F.Y., Chung S.L., Wilde S.A. & Chu M.F. 2004: Multiple sources for the origin of granites: geochemical and Nd/Sr isotopic evidence from the Gudaoling granite and its mafic enclaves, northeast China. *Geochimica et Cosmochimica Acta* 68, 4469–4483. https://doi.org/10.1016/j.gca.2004.04.015

Yazgan E. & Chessex R. 1991: Geology and tectonic evolution of the southeastern Taurides in the region of Malatya. *Turkish Association of Petroleum Geologists* 3, 1–42.

Yılmaz H., Alpaslan M. & Temel A. 2007: Two-stage felsic volcanism in the western part of the southeastern Anatolian orogen: petrologic and geodynamic implications. *International Geology Review* 49, 120–141. https://doi.org/10.2747/0020-6814.49.2.120

Yılmaz İ., Yılmaz Şahin S., Aysal N., Güngör Y. Akgündüz A. & Bayhanm U.C. 2021: Geochronology, geochemistry and tectonic setting of theCadomian (Ediacaran–Cambrian) magmatism in the Istranca (Strandja) Massif: new insights into magmatism along the northern margin of Gondwana in NW Turkey. *International Geology Review.* https://doi.org/10.1080/00206814.2021.1901249

Zhao P., Jahn B-M. & Xu B. 2017: Elemental and Sr-Nd isotopic geochemistry of Cretaceous to Early Paleogene granites and volcanic rocks in the Sikhote-Alin Orogenic Belt (Russian Far East): implications for the regional tectonic evolution. *Journal of Asian Earth Sciences* 146, 383–401. https://doi.org/10.1016/j.jseaes.2017.06.017

Electronic supplementary material is available online:

Table S1 at http://geologicacarpathica.com/data/files/supplements/GC-74-3-Erturk_Table_S1.xlsx
Table S2 at http://geologicacarpathica.com/data/files/supplements/GC-74-3-Erturk_Table_S2.xlsx
Table S3 at http://geologicacarpathica.com/data/files/supplements/GC-74-3-Erturk_Table_S3.xlsx
Table S4 at http://geologicacarpathica.com/data/files/supplements/GC-74-3-Erturk_Table_S4.xlsx